https://doi.org/10.5194/egusphere-2025-5374
Preprint. Discussion started: 16 December 2025

Dune aurora: Statistical survey from a citizen science database

Maxime Grandin[1], Liisa Juusola[1], Noora Partamies[2], Emma Bruus[3,4], Joona Rautiainen[3], Donna Lach[5], Jia Jia[1], Max van de Kamp[1], Eero Karvinen[4], Kirsti Kauristie[1], and Theresa Hoppe[1]

[1]Finnish Meteorological Institute, Helsinki, Finland
[2]Department of Arctic Geophysics, The University Centre in Svalbard, Norway
[3]Sodankylä Geophysical Observatory, University of Oulu, Sodankylä, Finland
[4]Skywarden observation system, Ursa Astronomical Association, Helsinki, Finland
[5]Aurorasaurus, New Mexico Consortium, Los Alamos, NM, USA

Correspondence: Maxime Grandin (maxime.grandin@fmi.fi)

Abstract. Auroral forms can provide information not only on the state of near-Earth space but also on conditions in the lower-thermosphere–ionosphere. The so-called dune aurora, consisting of brighter stripes forming a wave-like pattern in the dim, diffuse green aurora, has been hypothesised as being an optical signature revealing the presence of large-scale atmospheric waves above or near the mesopause. However, only a few dune aurora events have been studied to date, leaving many open questions regarding the nature of this phenomenon. We carry out the first statistical analysis of dune aurora events by collecting citizen science observations of the dunes since 2000 using the Skywarden (https://taivaanvahti.fi) database of observations. From a total of 289 dune aurora observations made during 56 different events by citizen scientists from Northern Europe, North America, Australia, and New Zealand, we investigate the distribution of dune events as a function of location, month, local time, solar wind and interplanetary magnetic field (IMF) conditions, and geomagnetic activity. We compare those distributions to that of all the aurora observations reported in Skywarden since 2000. We also estimate the duration of dune events based on the available observations, and we investigate a possible relationship between dune aurora and equivalent current patterns derived from ground-based magnetometer measurements. We find that the vast majority of dune observations take place near the equatorward boundary of the auroral oval, in the dusk sector earlier than the peak in all auroral report distribution, and in association with strong (in most cases eastward but occasionally westward) auroral electrojet signatures. The dune observations are often associated with elevated solar wind density and IMF magnitude, and the IMF B_y component may play a role in their formation. Finally, their monthly distribution peaks in March and October, which could be the result of a combination of geomagnetic, atmospheric, darkness, and cloudiness conditions needed for them to form.

1 Introduction

The interplay between the upper atmosphere and space is complex and remains to a great extent poorly understood. The lower-thermosphere–ionosphere is subject to forcing from space via, for instance, charged particle precipitation, electric currents flowing within the ionosphere–magnetosphere system, and high-latitude plasma drifts associated with magnetospheric convection (e.g. Palmroth et al., 2021; Sarris et al., 2023). This region is also affected by the underlying atmospheric layers from which upward propagating waves contribute to the neutral gas dynamics (e.g. Vadas and Liu, 2009; Vadas and Becker,

https://doi.org/10.5194/egusphere-2025-5374
Preprint. Discussion started: 16 December 2025

2019; Heelis and Maute, 2020). As measuring the properties of the lower-thermosphere–ionosphere is challenging, one way to indirectly obtain information on its state is to observe optical emissions coming from it. It has been shown, for instance, that the STEVE (Strong Thermal Emission Velocity Enhancement) phenomenon (MacDonald et al., 2018) is the optical signature of subauroral ion drifts (SAID; Archer et al., 2019), which are narrow channels of fast-flowing plasma in the thermosphere, difficult to measure in the absence of in situ satellite observations.

Another form of optical emission of particular interest to reveal upper-atmospheric dynamics is the dune aurora, which has also been referred to as "the dunes". The dunes are a diffuse auroral form exhibiting a wave pattern such that it forms bands of increased brightness roughly parallel to each other (see an example in Fig. 1). Like STEVE, the dunes were discovered thanks to citizen scientists. Using two pictures of the same dune display taken almost exactly at the same time, Palmroth et al. (2020) could determine that the auroral emission associated with the dunes was produced at approximately 100 km altitude, and that the region where they took place corresponded to that of the eastward electrojet. In a subsequent study, Grandin et al. (2021) found that dune aurora could span over 1500 km of horizontal distance (from western Finland to Scotland) and be visible for at least four hours. That study also revealed that the dunes were associated with 10–20 keV electron precipitation and a large temperature inversion layer below the mesopause. A possible role of precipitating protons was also discussed in that study, though more investigation is needed to examine their potential importance in the formation of dune aurora. In the few events that have been studied, the dune stripes exhibit a pseudo-wavelength ranging between 30 and 45 km (Palmroth et al., 2020; Grandin et al., 2021) and have an orientation roughly perpendicular to the auroral oval, although it is unclear whether this is always the case. In Grandin et al. (2021), the dunes were found to propagate at about $200\,\mathrm{m\,s^{-1}}$ with respect to the observer on the ground, in the westward direction.

The above elements suggest that the dunes may be the optical signature of an atmospheric wave propagating horizontally within diffuse aurora near the mesopause, as hypothesised in Palmroth et al. (2020). A candidate for such a wave could be the mesospheric bore (Dewan and Picard, 1998; Smith et al., 2003), whose properties (wavelength, propagation speed, altitude) are compatible with the observations reported in Palmroth et al. (2020) and Grandin et al. (2021). Mesospheric bores are known to form and propagate in presence of a ducting structure, which can be a temperature inversion layer in the mesosphere (thermal duct) or a wind shear below the mesopause (Doppler duct), as detailed in Dewan and Picard (2001). They are generally observed in airglow images and have been predominantly studied at low and midlatitudes (e.g. Hozumi et al., 2019). Their horizontal wavelength can range between 20 and over 100 km (Brown et al., 2004), and they typically have a spatial extent over several hundreds of kilometres. In some cases, a given mesospheric bore can contain over 15 trailing crests and troughs (Su et al., 2018). Recently, Chauhan et al. (2024) carried out a study of high-latitude mesospheric bores whose horizontal wavelengths ranged within 10–50 km for phase speeds within 20–100 $\mathrm{m\,s^{-1}}$. They found no correlation with auroral activity.

Besides mesospheric bores, it has been suggested that the dunes could be associated with acoustic waves. These would propagate within a non-linear periodic duct produced by meteor showers creating a dusty plasma around 100 km altitude (Izvekova et al., 2025). However, a totally distinct alternative hypothesis to explain the dune aurora's morphology involves a magnetospheric origin, with exohiss waves near the plasmapause spatially modulating the precipitating particle fluxes (He et al., 2023).

https://doi.org/10.5194/egusphere-2025-5374
Preprint. Discussion started: 16 December 2025

In the absence of conclusive evidence to confirm one of the hypotheses, there remain several open questions in relation to the dunes:

1. How frequent are the dunes, and are they associated with specific solar wind driving or geomagnetic activity conditions?
2. What is the distribution of the dune aurora as a function of geomagnetic latitude and magnetic local time (MLT)? Do they appear all year round, or is there a seasonality in their occurrence? What is the typical duration of a dune aurora event?
3. Do precipitating protons play a role in the formation of the dunes?
4. Are the dunes associated with the presence of an atmospheric wave near the mesopause? If so, is the mesospheric bore the most likely candidate wave?
5. Does the morphology of the dune aurora originate from magnetospheric processes?

Since the dunes have so far remained challenging to identify from all-sky camera images, a pathway to better understand them is to involve citizen science observations – that is, reports or photographs made by people who are not researchers by profession. Indeed, the narrower field-of-view of commercial cameras as typically used by aurora photographers is more suitable to reveal their presence in the diffuse aurora, especially since they tend to be more visible when viewed at relatively low elevations where structures in all-sky images are not easy to analyse. Auroral citizen science has recently gained significant momentum (see Grandin et al., 2025, for a recent review), especially boosted by the May 2024 extreme geomagnetic storm (e.g. Spogli et al., 2024; Grandin et al., 2024; Hayakawa et al., 2025; Lockwood et al., 2025).

This study presents the first statistical investigation of dune aurora observations combining 289 reports by citizen scientists from all around the world with measurements from scientific instruments. Section 2 describes the data sets and methods used in the study. Section 3 presents the results of the analysis in terms of spatio-temporal distribution of dune observations, their duration, their relation to solar wind driving and geomagnetic activity, and their association with ionospheric currents. Section 4 discusses the results, and conclusions are summarised in Section 5.

2 Data and methods

2.1 Citizen science observations from Skywarden

Skywarden (Taivaanvahti in Finnish, Himlakollen in Swedish; https://taivaanvahti.fi) is a database of observations of celestial phenomena (aurora, solar halos, deep-sky objects, noctilucent clouds, thunderstorms, eclipses, fireballs…) made by citizen scientists. It has been created, developed and maintained by the Ursa Astronomical Association in Finland. It was established in 2011 but it also includes a handful of historical observations which have been digitised recently; the oldest ones are a series of photographs of the aurora taken in Sodankylä in late 1927 – probably the oldest aurora photographs taken in Finland (Nevanlinna and Tanskanen, 2024). Skywarden has already proved useful as a database for studies investigating proton aurora

https://doi.org/10.5194/egusphere-2025-5374
Preprint. Discussion started: 16 December 2025

Figure 1. Example of dune aurora. The photograph was taken by Donna Lach on 9 November 2024 from the western shore of Lake Manitoba, Canada. The white rectangle indicates where the dunes are visible.

and stable aurora red arcs (Nishimura et al., 2022) as well as the May 2024 geomagnetic storm (Grandin et al., 2024; Lockwood et al., 2025).

We used the Skywarden Application Programming Interface (API) (Bruus, 2024) to search for observations made by citizen scientists during which dunes were identified. We carried out the search between 1 January 2000 and 30 June 2025, and restricted it to observations containing at least one photograph where the dunes were visible. We visually inspected all the events and determined the time intervals during which the dunes appeared in the pictures, either using the EXIF information contained in the images (if provided) or indications given by the observers in the free-text description of the observation. When no reliable time information can be retrieved but the dunes were clearly visible in at least one image, we retained the event but without giving it a time stamp (necessary to determine its magnetic local time and the associated driving and geomagnetic conditions). In total, we obtained 289 dune aurora observations, which were made during 56 different events by 178 named citizen scientists from Northern Europe, North America, Australia, and New Zealand (4 reports were anonymous).

https://doi.org/10.5194/egusphere-2025-5374
Preprint. Discussion started: 16 December 2025

In addition, we also collected all the aurora observations reported in Skywarden during the same time interval (1 January 2000 – 30 June 2025), to serve as a baseline when interpreting the seasonal and local time distributions of reported dune aurora events. To extract these data from Skywarden, we also used the API; we did not restrict the search to observations containing at least one picture in this case, nor did we visually inspect all the reports. In total, we obtained 15,382 aurora observation reports, which took place on 1808 individual days.

2.2 SuperMAG indices

For this study, we examined geomagnetic activity using two of the SuperMAG indices, calculated from ground-based magnetic measurements at 1 min time resolution by magnetometers from the SuperMAG network (Gjerloev, 2012). We used the SuperMAG Electrojet (SME) index (Newell and Gjerloev, 2011) as a measure of substorm activity, and the SuperMAG Ring current (SMR) index (Newell and Gjerloev, 2012) as a measure of geomagnetic storm activity. We downloaded the SME and SMR indices at 1 min resolution from January 2000 to June 2025.

2.3 OMNI data

We retrieved solar wind and interplanetary magnetic field (IMF) measurements at 1 hour time resolution between January 2000 and June 2025 from the OMNI database (Papitashvili and King, 2020). The OMNI data consist of solar wind parameters and IMF observations made by various spacecraft at the L1 Lagrange point of the Sun–Earth system and propagated to the Earth's bow shock, as well as selected geomagnetic indices (King and Papitashvili, 2005). For this study, we considered the following OMNI parameters: solar wind density, speed and dynamic pressure, as well as total IMF magnitude, and its B_y and B_z components in the Geocentric Solar Magnetospheric (GSM) coordinate system.

2.4 IMAGE data and calculation of equivalent ionospheric currents

We use 10 s resolution data from the International Monitor for Auroral Geomagnetic Effects (IMAGE) network to examine ionospheric equivalent currents associated with dune aurora observations. IMAGE currently consists of 57 ground-based magnetometers located in Fennoscandia and surrounding areas. It enables evaluating the ionospheric equivalent currents with a spatial resolution down to about 100 km, hence resolving the so-called mesoscale current structures. One method to derive equivalent currents, known as the Spherical Elementary Current System method (SECS), was introduced in Amm (1997) and has been widely used since then (e.g. Vanhamäki and Juusola, 2020).

3 Results

3.1 Geographic, monthly, and local time distributions of dune events

Figure 2 shows an overview of all the dune observations reported to Skywarden between January 2000 and June 2025. In practice, the earliest observation available at the time of this study was made in 2004, and it is the only one prior to January

https://doi.org/10.5194/egusphere-2025-5374
Preprint. Discussion started: 16 December 2025

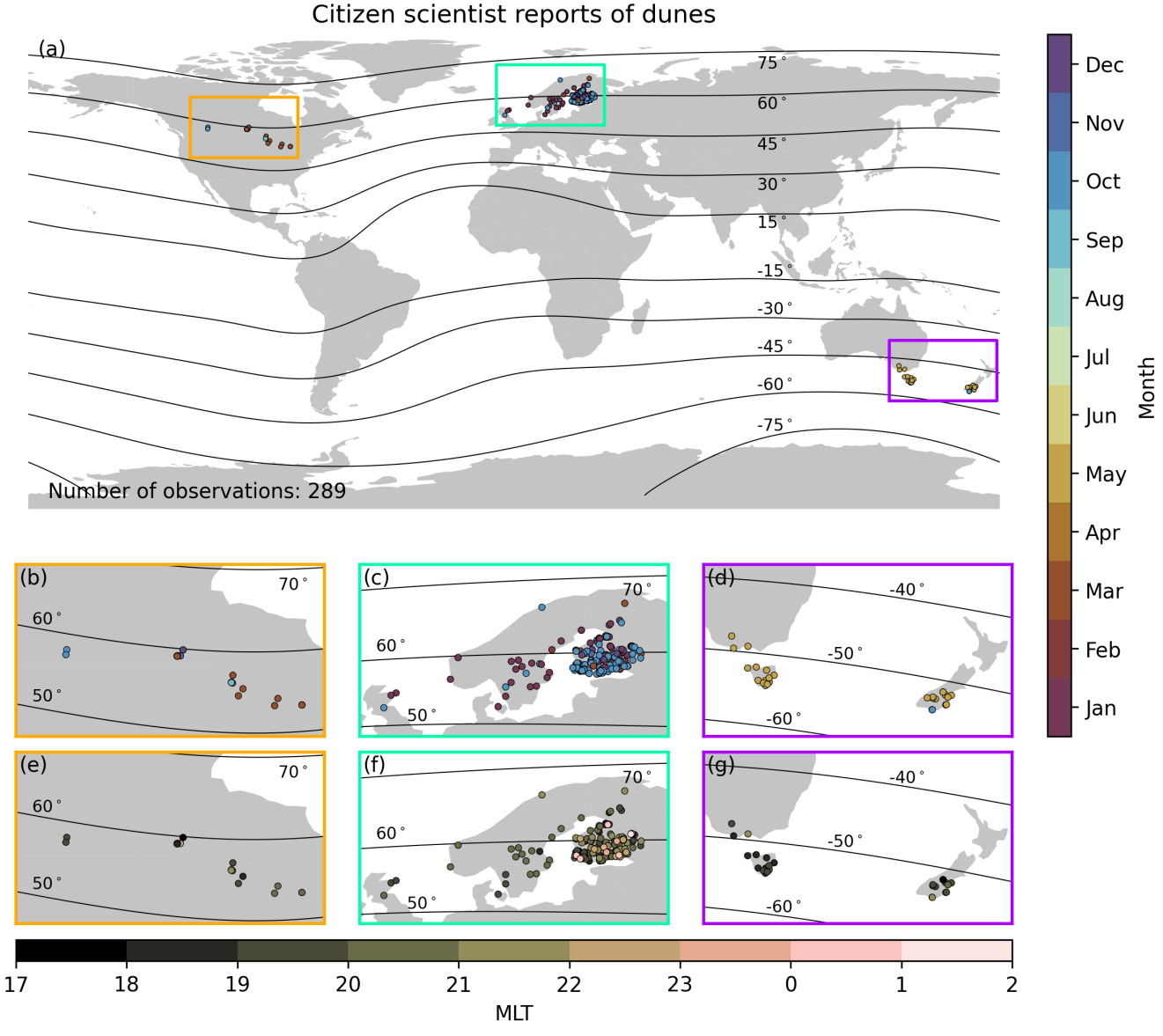

Figure 2. (a) Overview of the reported dune observations around the world. The colour of the dots indicates the month when the corresponding observation took place. Zoom-in with the same colour code over (b) North America, (c) Northern Europe, and (d) Australia and New Zealand. (e–g) Zooms-in over the same three regions but with dots coloured according to the MLT of the dune observations. The black lines indicate geomagnetic latitude isocontours, obtained from the AACGM-v2 library (Shepherd, 2014).

https://doi.org/10.5194/egusphere-2025-5374
Preprint. Discussion started: 16 December 2025

2014. The time span of more frequent dune observations still covers approximately one solar cycle. In Fig. 2a–d, the colour of the dots indicates the month when the observation took place.

The dune aurora reports come from three main regions (by decreasing number of observations): Northern Europe, Australia and New Zealand, and North America. These regions have particularly active aurora chaser groups exchanging knowledge and information via social media pages. These groups contribute to Skywarden – but also to other platforms such as Aurorasaurus (MacDonald et al., 2015) – with their observations. In the North American sector, there are a few observations from Manitoba, Alberta, and Michigan made during the northern-hemisphere autumn, winter, and spring. In the European sector, while the vast majority of reports come from Finland, there is also a number of them from Sweden, and a couple from Norway, Denmark, and Scotland. Most observations were made during the northern-hemisphere autumn and winter, and a few of them in early spring. In New Zealand and Australia, almost all observations were made in May; these correspond to the May 2024 geomagnetic storm. In all three sectors, dune aurora observations were predominantly made near or below 60° geomagnetic latitude, that is, at subauroral latitudes.

Figures 2e–g show the same observations but with dots coloured according to the magnetic local time (MLT), calculated with the AACGM-v2 Python library (Shepherd, 2014; Burrell et al., 2020). When it was not possible to determine accurately enough the time stamps in a given Skywarden observation (this is the case for 28 observations), the MLT was not calculated, and the corresponding observations are not shown in these figures. When multiple dune images were included in a given observation report, or when the observer provided the time interval during which they photographed dune aurora, we retain the earliest time with a dune image to calculate the MLT.

While MLT hours range from 17.5 to 1.2 across dune observations, one can see that most observations were made in the pre-midnight sector. More insight on the MLT distribution of dune events is given in Fig. 3a. It is clear that the large majority of dune observations were made between 18 and 22 MLT, with a peak around 20 MLT. The apparent asymmetry in the distribution, with the longer tail towards dawn, is likely due to the lack of observations during afternoon daylight.

In Fig. 3b, we show the monthly distribution of individual dune events. A dune event is defined such that observations that took place on the same day and within the same longitude sector (within 40°) are considered forming part of the same dune event. This results in a total of 56 dune events, whose monthly distribution exhibits a peak in October, another one in March, and contains several events in the other months of the northern-hemisphere winter and early spring (November to April). There are only a couple of events in May, August, and September, and no events in June and July.

Citizen science observations are not continuous and bear some bias related to the typical human behaviour, such as staying awake past sunset, sleeping at night, and waking up around or after sunrise. As it is known that the occurrence rate of auroras is not evenly distributed throughout the year, we compare the MLT and monthly distributions of dune observations/event with a baseline given by all the available aurora observations from Skywarden. Figure 3c shows the MLT distribution of the 15,382 aurora observation reports retrieved between January 2000 and June 2025. While it is clear that most aurora observations took place in the pre-midnight sector, the peak of the distribution is found around 22 MLT, i.e. two hours later than that of the dune observations. This indicates that the dunes are predominantly a pre-midnight phenomenon, with an increased likelihood to occur in the few hours after 18 MLT. The monthly distribution of all aurora event dates is given in Fig. 3d. Here, for simplicity,

https://doi.org/10.5194/egusphere-2025-5374
Preprint. Discussion started: 16 December 2025

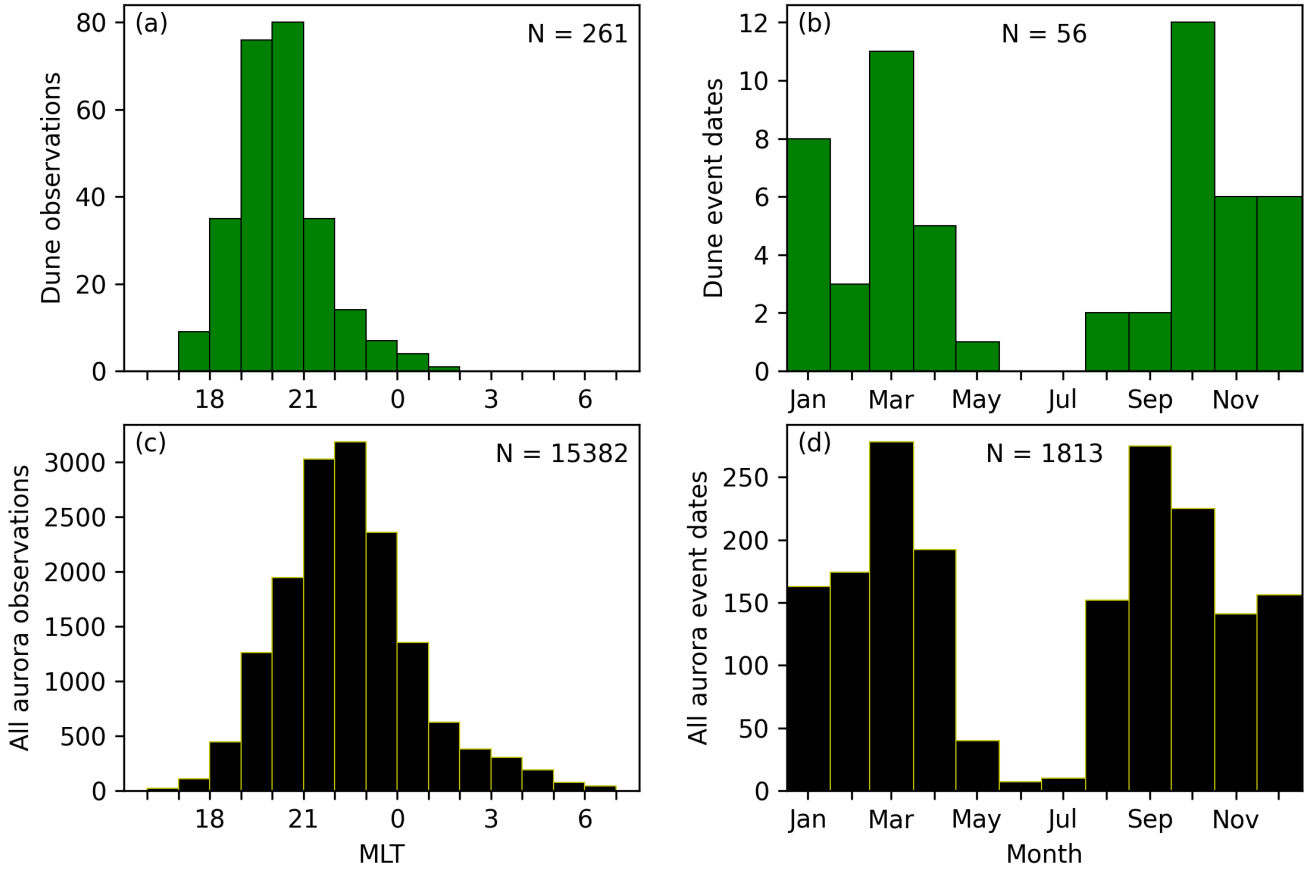

Figure 3. (a) MLT distribution of the dune observation start times. (b) Monthly distribution of individual dune aurora events. (c) MLT distribution of all aurora observation start times. (d) Monthly distribution of individual days with aurora observations in Skywarden.

we simply retain individual days with at least one aurora report in Skywarden without considering the longitudes, such that, for instance, the 11 May 2024 is counted only once.

The histogram reveals two peaks around the equinoxes (March and September). Notably, 69% of dunes events and 95% of all aurora events in Skywarden were observed in Finland. This highlights the importance of analysing local observation conditions, such as cloudiness and darkness conditions, when interpreting the monthly distribution of observed events. In Appendix B, Fig. B1 shows the monthly average of cloudiness in Finland, obtained from the Finnish Meteorological past weather database.

Across Finland, the average cloudiness during the darkest winter months (from November to January) typically ranges between 6 and 7 okta, whereas observing conditions are better in spring (March and April) and early autumn (September). This likely explains to a great extent the peaks in auroral observations reported in Skywarden in March and September (Fig. 3), in

https://doi.org/10.5194/egusphere-2025-5374
Preprint. Discussion started: 16 December 2025

addition to the Russell–McPherron effect (Russell and McPherron, 1973) which leads to enhanced geomagnetic activity during equinoxes.

Besides, the deep trough in dune and auroral observations between May and July is due to the fact that, during that period of the year, nights are not dark enough in Finland for the aurora to be visible. Given that the vast majority of the reports in Skywarden are from Finland, this effect greatly shapes the monthly distributions shown in Fig. 3b and 3d.

Interestingly, September is a month for which only two dune aurora events have been recorded (Fig. 3b), whereas the largest dune event occurrence peak is in October (12 events). The majority of dune events in October were observed in Finland, which has a monthly average nighttime cloudiness close to 6 okta (in comparison, for September it is under 5 okta). These relatively unfavourable observation conditions suggest that it is likely that recorded events contain only a fraction of all dunes events occurring in October. We also note a low number of dune events in February, not reflected in the all-aurora distribution. If not simply due to too small a number of events for the monthly statistics to be robust, the dominance of October and relative lack of dune events in February and September may suggest that the dunes require conditions that are not only related to geomagnetic activity. A possible factor leading to a lower number of dune events in September compared to October is the fact that the early evening hours, when the dunes are typically observed, are not dark in early September. The fact that equinoxes occur around 20 March and 23 September rather than in the middle of those months implies that evening hours are slightly darker in March than in September, hence making it more favourable for the dunes to be observed in March than in September. Nevertheless, this bias in darkness conditions cannot alone explain the low number of dune events in September, as April – when the Sun sets at later hours than in September – has noticeably more dune events than September. Hence, the September–October difference in dune event number might also, for instance, have something to do with atmospheric dynamics which have their own seasonal patterns.

3.2 Dune event duration

Citizen scientist observations of the aurora are not continuous and hence they are unlikely to capture the dune events in their entirety. However, the large database provided by Skywarden observations enables us to determine conservative lower-boundary estimates of dune observation durations, when either multiple photographs are appended to the Skywarden record or the observer indicated in the description text within which time range they have dunes in their images. Out of the 289 Skywarden dune observations used in this study, this is the case for 140 of them.

Figure 4a gives the distribution of dune observation durations as determined from individual Skywarden reports. While approximately a third of them (49/140) were photographed for less than 15 min, the distribution exhibits a gradual decrease with increasing durations, including a non-negligible tail beyond 1 h amounting to about 15% (22/140) of the observations. Two observations included dune photographs for more than three hours; one was reported from Finland on 23 October 2022 (3.2 h), and the other one from Tasmania on 11 May 2024 (4.2 h). Multiple factors need to be met for the totality of a dune display to be recorded by a single observer. For instance, the observer needs to be photographing before the dunes appear and until they have vanished, and they need to keep the camera pointed in the direction of the dim dune aurora rather than turn it towards brighter and more dynamical auroral structures. Therefore, we consider the distribution shown in Fig. 4a a lower-

https://doi.org/10.5194/egusphere-2025-5374
Preprint. Discussion started: 16 December 2025

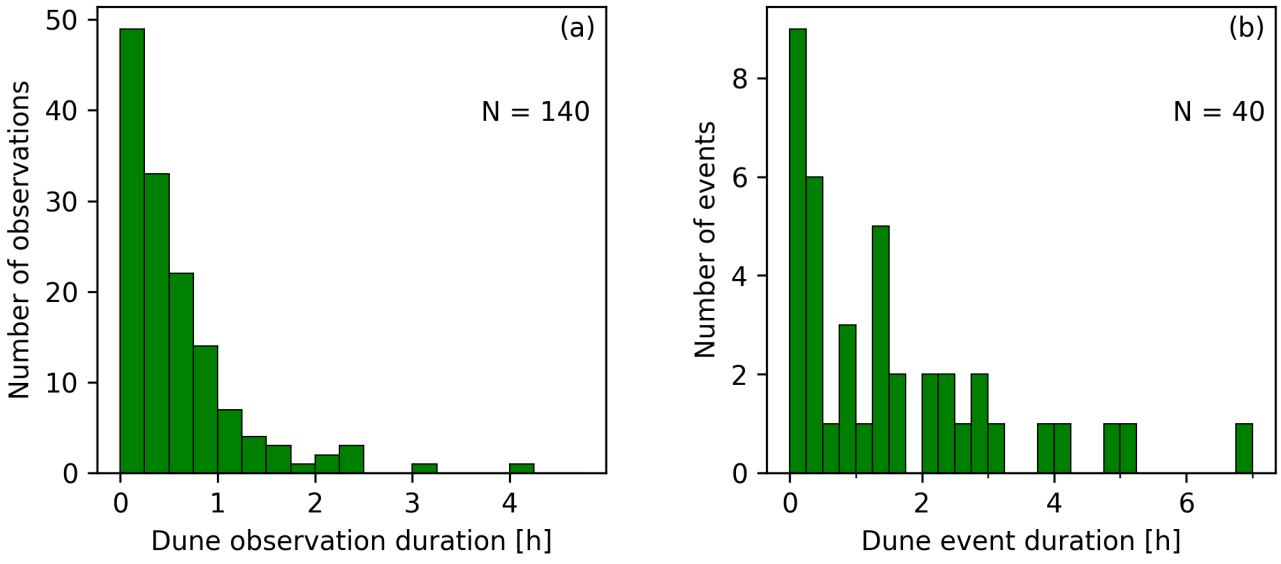

Figure 4. Distributions of the duration of (a) dune observations (i.e. by a single observer), and (b) dune aurora events (i.e. combining multi-observer observations of the same event). These are conservative lower-boundary estimates based on the information available in the Skywarden observation logs.

boundary estimate of the true duration of the corresponding dune events. To get a more comprehensive overview of the duration of dune events, we can combine the information contained in multiple observations of the same event. Figure 4b shows the distribution of dune event durations based on multiple (when available) reports by observers. Only dune events for which either several reports were made or a single report containing information on the duration of dune presence in images are shown in the figure. This is the case for 40 out of the 56 dune aurora events considered in this study. We can see that only half of the events (19/40) have a duration less than an hour, 20% (8/40) of them were photographed for between one and two hours, and about a third of them (13/40) have been recorded for more than two hours. Five events are of particularly long duration: the 7 October 2015 event observed from Finland and Scotland (3.8 h); the 17 December 2023 event observed from Finland (4.1 h); the 13 March 2022 event also observed from Finland (4.8 h); the 20 January 2016 event observed from Finland, Norway, and Scotland (5.2 h); and the 11 May 2024 event observed from New Zealand and Australia (6.9 h). This confirms that dune aurora can cover a wide region and last for multiple hours, as was noted in Grandin et al. (2021).

3.3 Distribution of dunes as a function of solar wind and geomagnetic activity

Only three percent of recorded aurora events presented dunes. To assess whether dune aurora is associated with specific solar wind driving conditions, we compare the distribution of selected solar wind and IMF parameters (solar wind density, speed, dynamic pressure, IMF magnitude, and IMF B_y and B_z components in the Geocentric Solar Magnetospheric coordinate system) associated with dune observations and associated with all the aurora observations from Skywarden. This is shown in

https://doi.org/10.5194/egusphere-2025-5374
Preprint. Discussion started: 16 December 2025

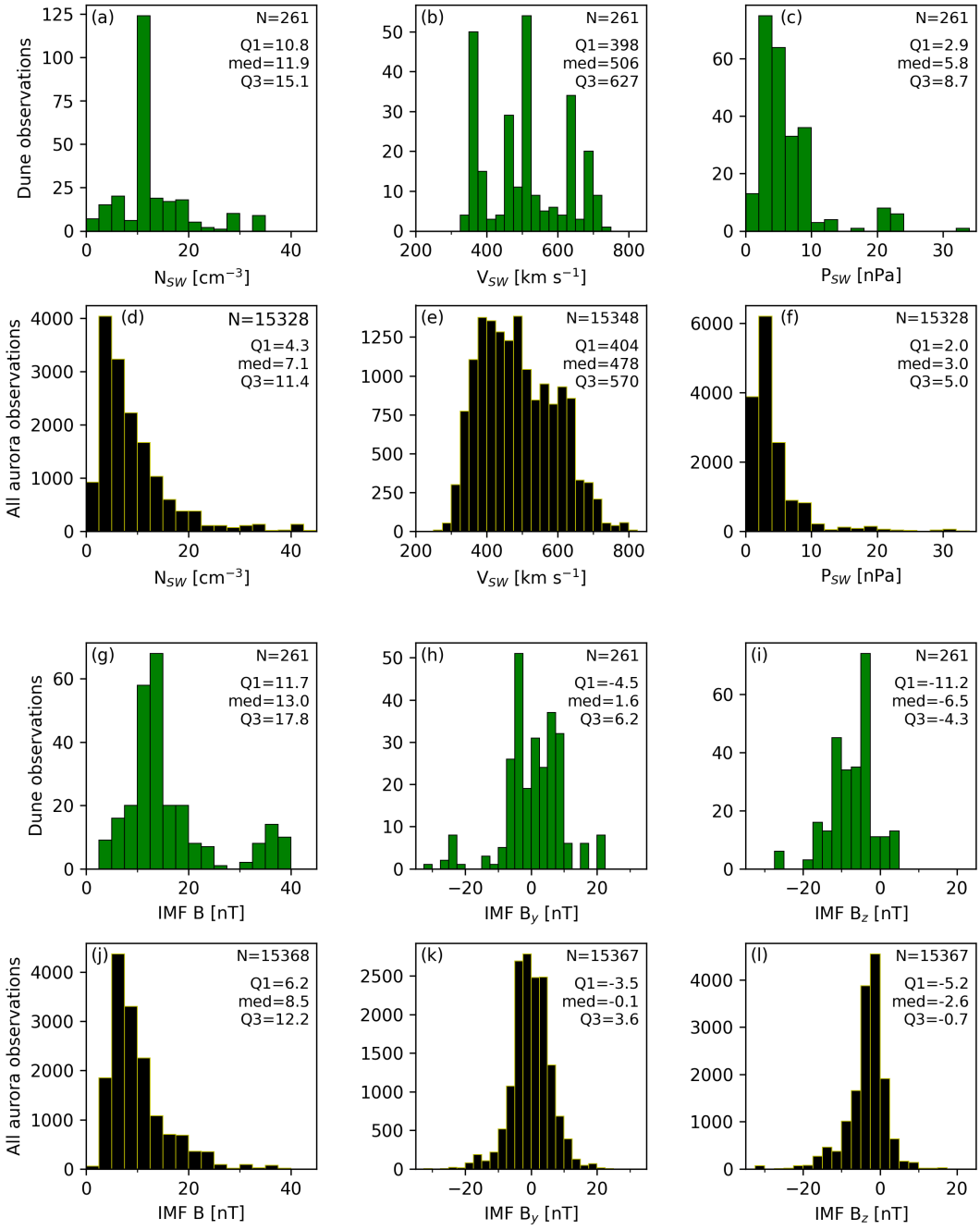

Figure 5. Solar wind and IMF parameters associated with dune observations (green histograms) and all aurora observations (black histograms). The considered parameters are: (a,d) solar wind density; (b,e) solar wind speed; (c,f) solar wind dynamic pressure; (g,j) IMF magnitude; (h,k) IMF B_y component; and (i,l) IMF B_z component.

https://doi.org/10.5194/egusphere-2025-5374
Preprint. Discussion started: 16 December 2025

Fig. 5, where histograms corresponding to dune observations are given in green whereas those for all aurora observations are in black. The total number of data points is given in the top-right-hand corner of each panel, as are the values of the lower quartile, median, and upper quartile.

For every Skywarden report, the driving parameters were retrieved from the 1 h OMNI data. We retain the average between the value of each parameter two hours and one hour prior to the start time of the observation (that is, two values), to account for the time delay between the arrival of the measured solar wind and IMF at the Earth's bow shock (as given by OMNI data) and their effects in the magnetotail (e.g. Rong et al., 2015; Pitkänen et al., 2016)

Looking at Fig. 5a–f, it appears that dune aurora observations tend to take place when solar wind driving is stronger than during typical aurora observations. Dune aurora events occur when the solar wind density is elevated: the lower quartile of the solar wind density during dune observations is almost equal to the upper quartile of that during all aurora observations. The difference is less striking when it comes to the solar wind speed and dynamic pressure, but dune aurora distributions have higher values than all-aurora ones for these two parameters too.

Regarding the IMF, we note that the total magnitude distributions exhibit a similar situation as the solar wind density, with the lower quartile for dune observations (Fig. 5g) being almost equal to the upper quartile for all aurora observations (Fig. 5j). While the distribution of IMF B_y values for all aurora observations is remarkably centred and symmetrical (Fig. 5k), for dune observations we observe a dip within the range of near-zero values and two peaks near $B_y = \pm 5$ nT (Fig. 5h). The median value around +1.6 nT suggests a possible slight favouring of positive B_y values, which generally brings the Harang discontinuity to the evening sector and strengthens the westward electrojet in the wintertime northern hemisphere (Holappa et al., 2021). Such IMF B_y effects have been shown to maximise at subauroral latitudes (Holappa et al., 2019). Finally, IMF B_z values are overall more strongly negative during dune observations (Fig. 5i) than for all aurora observations (Fig. 5l).

Next, we examine the distribution of dune aurora observations with respect to geomagnetic latitude, together with geomagnetic activity as measured with the SME and SMR indices. Figure 6a shows the geomagnetic latitudes of dune observations as a function of time, with red stars corresponding to northern-hemisphere latitudes and blue stars corresponding to southern-hemisphere latitudes. This way of displaying the data enables one to visualise the latitudinal spread of dune observations during individual events. We can see for instance observations spanning more than 5° in geomagnetic latitude during the 7 October 2015 event (57.2–64.0°N), the 7 October 2018 event (55.4–60.4°N), the 14 January 2022 event (54.0–63.9°N), the 17 December 2023 event (57.6–63.7°N), and the 11 May 2024 event (47.9–54.4°S). This highlights how widespread the dunes may be during some events. In Fig. 6b, the same data are displayed as a histogram, peaking at latitudes a few degrees below 60°. For comparison, the geomagnetic latitude distribution of all aurora observations retrieved from Skywarden is shown in Fig. 6c. While it is difficult to assess whether the fact that this distribution peaks slightly polewards from that of the dune observations is significant, we note that it contains a more prominent tail beyond 60°. Keeping in mind that these distributions are certainly biased by the over-representation of observations from southern Finland compared to other regions of the world, this is consistent with the hypothesis that dunes may be a subauroral zone phenomenon.

Figures 6d–i present, in a similar format as the above panels, the distribution of the SME and SMR indices during the dune and all-aurora observations. These two indices are measures of substorm and geomagnetic storm activity as they are proxies

https://doi.org/10.5194/egusphere-2025-5374
Preprint. Discussion started: 16 December 2025

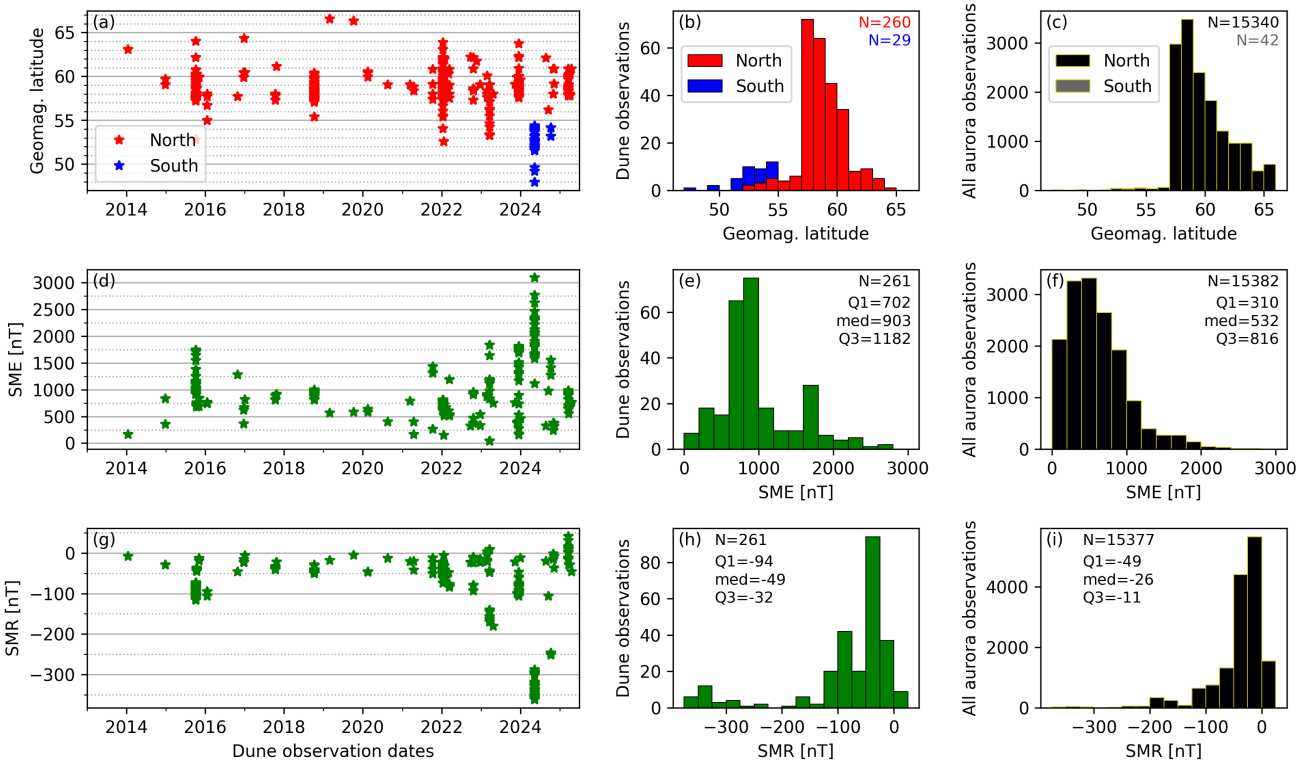

Figure 6. (a) Geomagnetic latitude of dune observations as a function of the observation dates, and (b) corresponding distribution. Northern-hemisphere latitudes are shown in red and southern-hemisphere latitudes (projected to the northern hemisphere) in blue. (c) Geomagnetic latitude distribution of all aurora observations; northern-hemisphere latitudes are shown in black and southern-hemisphere latitudes in grey. (d) SME index of dune observations as a function of the observation dates, and (e) corresponding distribution. (f) SME index distribution of all aurora observations. (g–i) Same for the SMR index.

for auroral electrojet and ring current, respectively. Since SuperMAG indices are provided at 1 min temporal resolution, and given that the aurora observations do not have such a high temporal resolution, we retain a 30 min average of the SME and SMR indices around the start time of each observation (i.e., between 15 min before and 15 min after that time stamp). The main results that can be inferred from these figures are the following:

1. During a dune event, SME and SMR values can change significantly (see Figs. 6d,g). This implies that the dunes span across not only a large geographic zone as discussed above, but also during a significant time interval. This is consistent with the findings from Fig. 4 that dune events can last for up to several hours, a time over which SME and SMR can vary significantly.

https://doi.org/10.5194/egusphere-2025-5374
Preprint. Discussion started: 16 December 2025

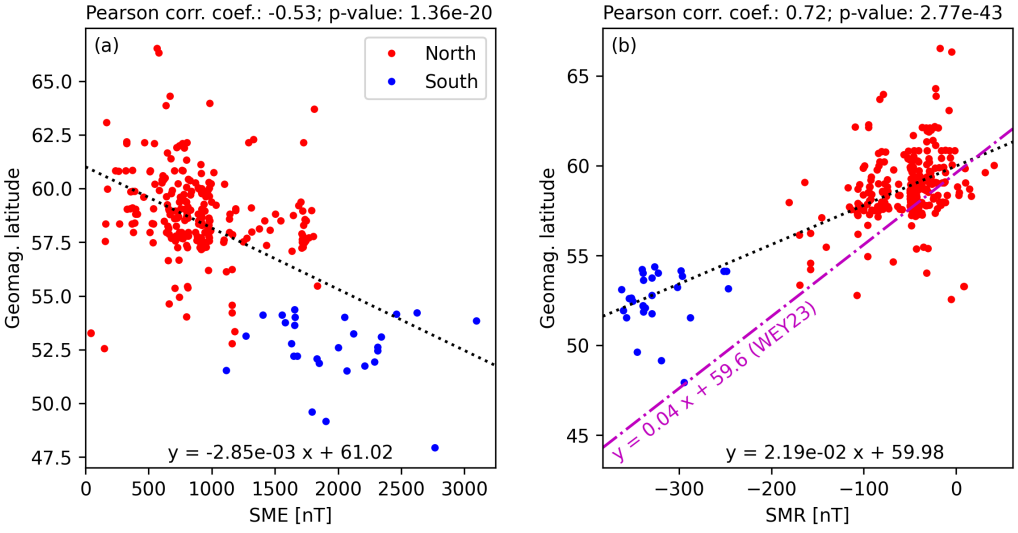

Figure 7. (a) Scatter plot of the geomagnetic latitude of dune observations as a function of the SME index. Blue dots correspond to southern-hemisphere observations and red dots to northern-hemisphere observations. The dotted line shows the linear regression of the data points; its equation is given at the bottom of the panel. The corresponding Pearson correlation coefficient and p-value are given above the panel. (b) Same for the geomagnetic latitude of dune observations as a function of the SMR index. The dash-dotted magenta line shows an approximate parametrisation of the auroral oval boundary adapted from Weygand et al. (2023).

2. Generally, the dunes are seen when auroral electrojet intensity is elevated (50% of the observations were made with SME within 702–1182 nT; see Fig. 6e). It however does not need to be extreme, as the median value of SME is 903 nT, but it is significantly higher than the median value of SME for all aurora observations (532 nT, Fig. 6f).

3. Likewise, the dunes tend to be observed when geomagnetic activity is enhanced (median SMR value: –49 nT; see Fig. 6h), though they do not require a strong geomagnetic storm for which a threshold of –100 nT is generally retained (e.g. Gonzalez et al., 1994; Zhang et al., 2008; Nitta et al., 2021). We note however that, if the dunes do appear during a geomagnetic storm, this analysis does not assess whether the threshold of –100 nT is attained at any point during the storm, before or after the dune observations. Still, the distribution of SMR index values associated with dune observations is skewed towards more strongly negative values than that obtained by considering all aurora observations (Fig. 6i).

Finally, we investigate a possible correlation between the dune aurora observations' geomagnetic latitude and geomagnetic activity. Figure 7 shows the relationship between geomagnetic latitude of the dune observations and the SME (Fig. 7a) and SMR (Fig. 7b) indices. Here too, northern hemisphere observations are represented in red and southern hemisphere observations in blue. In both panels, we calculated linear regressions between geomagnetic latitude and the SuperMAG indices; the linear fit curve is shown as a dotted black line and its equation is given below the data points. We also indicate the Pearson correlation coefficient and the p-value associated with the linear regression.

https://doi.org/10.5194/egusphere-2025-5374
Preprint. Discussion started: 16 December 2025

In both cases, the obtained p-value is very close to zero, indicating that the relation between the geomagnetic latitude of observations and the considered SuperMAG index is not coincidental. With SME, the geomagnetic latitude of dune observations is negatively correlated with a Pearson correlation coefficient of –0.57, whereas for SMR the correlation is positive with a Pearson correlation coefficient of 0.74. These values can be interpreted as demonstrating a moderately significant correlation, although we note that the observations associated with extreme SME and SMR value were all made during the May 2024 geomagnetic storm and come from the southern hemisphere, which might imply that the apparent correlations would be weaker without this event.

Nevertheless, phenomenologically, in the case of SMR, such a correlation is consistent with the expansion of the auroral oval which reaches lower latitudes as SMR becomes more strongly negative. The dash-dotted magenta line in Fig. 7b shows an approximate parametrisation of the auroral oval equatorward boundary adapted from Weygand et al. (2023), who calculated a linear regression of the boundary of the region 2 currents in the midnight MLT sector as a function of the SYM-H index, during six geomagnetic storms. Assuming that SYM-H and SMR do not differ significantly from each other, we applied the same slope and intercept using the SMR index to obtain a proxy for the auroral oval's equatorward boundary. While our linear fit of dune observation geomagnetic latitudes as a function of SMR (dotted black line) shows differences with that approximate oval boundary parametrisation, both curves are relatively close to each other, especially for moderate-to-strong geomagnetic storms (SMR > –200 nT) like those considered by Weygand et al. (2023). Besides the use of a different ring current index in the parametrisation, we should also keep in mind that differences are expected, as the majority of dune aurora observations occur in the dusk-to-premidnight sector rather than near magnetic midnight where the Weygand et al. (2023) linear regression was derived. Finally, differences may also be expected from the fact that the majority of the Skywarden observations are from Finland, where the Baltic sea imposes a cutoff of observations at about 57.5° geomagnetic latitude, whereas Weygand et al. (2023) obtained their parametrisation using observations in the Canadian sector, where no such lower-latitude cutoff exists.

For SME, the interpretation of a possible correlation is a bit less straightforward, but it likely stems from the fact that stronger storm conditions are often associated with higher substorm activity (Partamies et al., 2013), hence elevated substorm activity is also needed for the dunes to be visible from lower latitudes.

3.4 Equivalent currents associated with dune aurora

In the study of the first dune event by Palmroth et al. (2020), it was noted that the dunes occurred in concert with a strong eastward electrojet. Here, we leverage the larger dune event database provided by Skywarden reports to assess whether this is a typical situation for all dune events.

We first identify the dune events for which several clear dune observations have been made in the same geographic area, such that we have an indication of a nonzero time period over which the dunes were photographed. We only retain dune observations from the Fennoscandian sector, where ground-based magnetometers from the IMAGE network are close enough to each other to resolve mesoscale patterns (that is, ∼100 km horizontal scales) in equivalent currents. When a very large number of observations across a broad area was available for a given event, the observations have been separated into subgroups according to their geographic longitude. We obtain 17 events for which the equivalent current analysis can be carried out.

https://doi.org/10.5194/egusphere-2025-5374
Preprint. Discussion started: 16 December 2025

Table 1. Equivalent current analysis of dune aurora events having several observations. For each event, we indicate the number of observations retained and the geographic coordinates of their barycentre. We examine whether the dunes are associated with the eastward (E) or westward (W) electrojet (an arrow indicates a transition from one to the other) and if they take place near the Harang discontinuity. The events shown in Fig. 8–10 are marked with †.

Event date and time (UTC)	Number of observations	Mean coordinates of observations (geogr.)	Associated electrojet	Harang discontinuity
2015-10-07 15:58–18:43	16	61.2N, 22.8E	E → W	Present
2015-10-07 17:01–18:37	12	62.5N, 28.2E	E → W	Present
2015-10-12 18:09–18:34	5	61.5N, 22.9E	E	Present
2016-01-20 17:07–17:37	2	60.6N, 22.5E	E	Present
2017-10-13 16:30–17:53	3	60.8N, 24.6E	E	Present
2018-10-07 17:15–18:05	17	61.1N, 23.6E	E	Present
2018-10-07 17:27–18:04	12	61.8N, 26.7E	E	Present
2022-01-14 18:33–20:41	22	62.4N, 26.6E	E	Present
2022-01-14 18:42–20:40	12	62.6N, 23.9E	E	Present
2022-01-14 19:00–21:32†	11	60.5N, 15.6E	E → W	Present
2022-10-22 17:05–19:24†	2	60.8N, 16.0E	E	Present
2022-10-23 16:34–19:45	3	63.3N, 27.5E	E → W	Present
2023-02-26 20:45–21:07	4	61.4N, 24.9E	W	Present
2023-03-23 18:41–18:47†	2	61.2N, 23.0E	W	Present
2023-12-17 15:29–17:35	9	61.1N, 23.2E	E	Present
2023-12-17 15:34–16:53	12	62.7N, 26.2E	E	Present
2023-03-21 19:15–20:41	9	62.0N, 26.9E	E	Present

Table 1 summarises the results of the equivalent current analysis. The first column gives the date and time interval within which the dunes were photographed during the retained observations. The second column indicates the number of observations, for which the mean geographic coordinates are given in the third column. The fourth and fifth columns indicate whether the dunes were observed in conjunction with the eastward (E) or westward (W) electrojet and with the Harang discontinuity, respectively. This was assessed by visual inspection of the equivalent current figures, some examples of which are given in Fig. 8–10.

In practice, for each set of observations, the SECS analysis method is carried out using all the available IMAGE stations. The results are presented in the form of keograms of the geographic east (ϕ) and south (θ) components of the yielded equivalent current density ($\boldsymbol{J}_{\mathrm{eq}}$) as a function of time and geographic latitude, for the longitude of the dune observations, as exemplified in Fig. 8a–b for the 14 January 2022 event observations from the Swedish sector. Additionally, equivalent current maps can be displayed (see Fig. 8c), wherein horizontal current direction and magnitude are indicated with black arrows and the curl

https://doi.org/10.5194/egusphere-2025-5374
Preprint. Discussion started: 16 December 2025

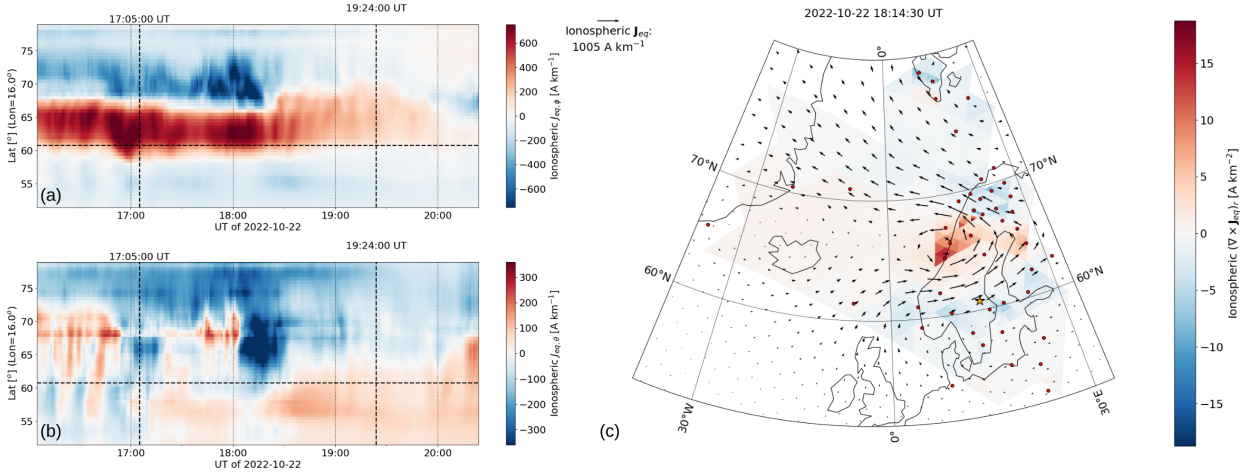

Figure 8. Equivalent current analysis applied to dune observations in the Swedish sector during the 22 October 2022 event. (a) ϕ (positive eastwards) component of the equivalent currents. The horizontal dashed line indicates the average geographic latitude of the dune observations; the vertical dashed lines indicate the earliest and latest dune observations. (b) θ (positive southward) component of the equivalent currents. (c) Map of the equivalent currents at 18:14 UT. The colour scale indicates the curl of the calculated equivalent currents, with positive (negative) values being a proxy for upward (downward) field-aligned currents. The arrows indicate the direction and magnitude (scale given in the top-left corner of the panel) of the horizontal currents. The yellow star shows the mean location of the retained dune observations, and magnetometer stations used in the SECS analysis are shown with red dots.

of the equivalent currents, which is a proxy for field-aligned current density (e.g., Weygand and Wing, 2016), is shown as the background colour. In the following, we look in more detail at such results for three selected events exemplifying the three configurations with respect to the eastward and westward electrojets.

It appears from Table 1 that there are three types of situations when it comes to the coincidence of the dune aurora with the auroral electrojets. In 11 cases, the dunes are found to occur within the eastward electrojet, like in Palmroth et al. (2020). However, in two cases, they are taking place within the westward electrojet, and in the remaining four cases they start within the eastward electrojet but remain visible throughout the transition to the westward electrojet. Besides, all events appear to take place in the vicinity of the Harang discontinuity.

Figure 8 shows an example of a set of dune observations associated with the eastward electrojet and a clear Harang discontinuity. In Fig. 8a and 8b, the keograms have been obtained along the meridian whose longitude corresponds to the average of the observers' longitudes. Note that the horizontal line appearing around 68° latitude in Fig. 8b is an artifact produced by the analysis, which does not affect the region we are interested in here. The mean geographic latitude of observers' locations is indicated with a horizontal dashed line, and the two vertical dashed lines mark the earliest and the latest dune photograph from that set of observations, respectively. Throughout the time interval during which dunes have been photographed from Sweden, the observers are close to the equatorward edge of the eastward electrojet. It is important to note that the dunes may have been present before the earliest reported observation and after the latest one, and that it is also possible that the dunes were not

https://doi.org/10.5194/egusphere-2025-5374
Preprint. Discussion started: 16 December 2025

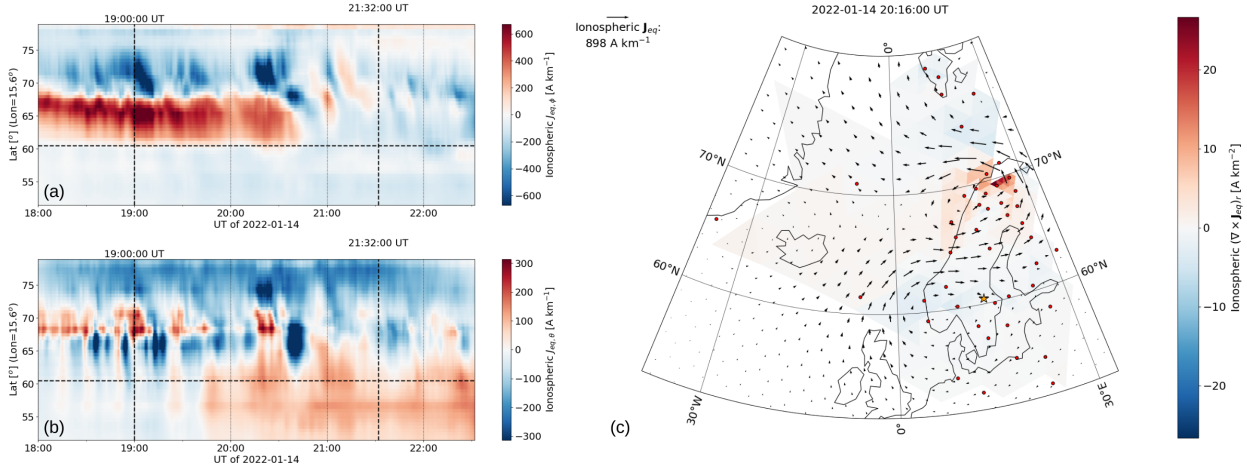

Figure 9. Equivalent current analysis applied to dune observations in the Swedish sector during the 14 January 2022 event. Same format as Fig. 8.

necessarily visible at all times during the marked time interval. We note interesting pseudo-periodic features in the eastward component of the equivalent currents (Fig. 8a) starting around 18:20 UTC, possibly indicating northward propagating current structures arising near the equatorward edge of the eastward electrojet. Similar signatures can be seen in a few other events, and it is unclear how they are generated and to what extent they may be related to the dune aurora.

Figure 8c shows the equivalent current map at the time of the earliest photograph of the set of observations. The large-scale features of the reconstructed equivalent currents clearly exhibit a well-delimited and relatively strong (scale shown in the top-left corner of the panel) eastward electrojet between the region-1 (upward, in red) and region-2 (downward, in blue) field-aligned currents. Near the eastern edge of the resolved area, the reversal in the horizontal current direction with increasing latitude indicates the presence of the Harang discontinuity.

In a few cases, the dune observations start within the eastward electrojet but continue after transitioning to the westward electrojet. An example of such events is given in Fig. 9 with the observations of the 14 January 2022 event within the Swedish sector. The eastward component of the equivalent currents near the observers' mean location (Fig. 9a) is positive until ∼20:40 UT, after which it is negative, corresponding to a westward current. We note that the last reported observation of dunes in the sector (at 21:32 UT, vertical dashed line) seems to match the disappearance of a patch of eastward current at high latitudes (above 65°). This might however be a mere coincidence. Figure 9c shows the equivalent current map at 20:40 UT. A clear Harang discontinuity signature can be seen polewards from the observers' mean location (yellow star).

Finally, an example of dune observations reported in conjunction with the westward electrojet is given in Fig. 10. Only two observers from Finland shared photographs of the event, which took place on 23 March 2023 and had observations only during a brief time interval (6 min). The SECS analysis unambiguously indicates that, at the time of those observations, the Finnish

https://doi.org/10.5194/egusphere-2025-5374
Preprint. Discussion started: 16 December 2025

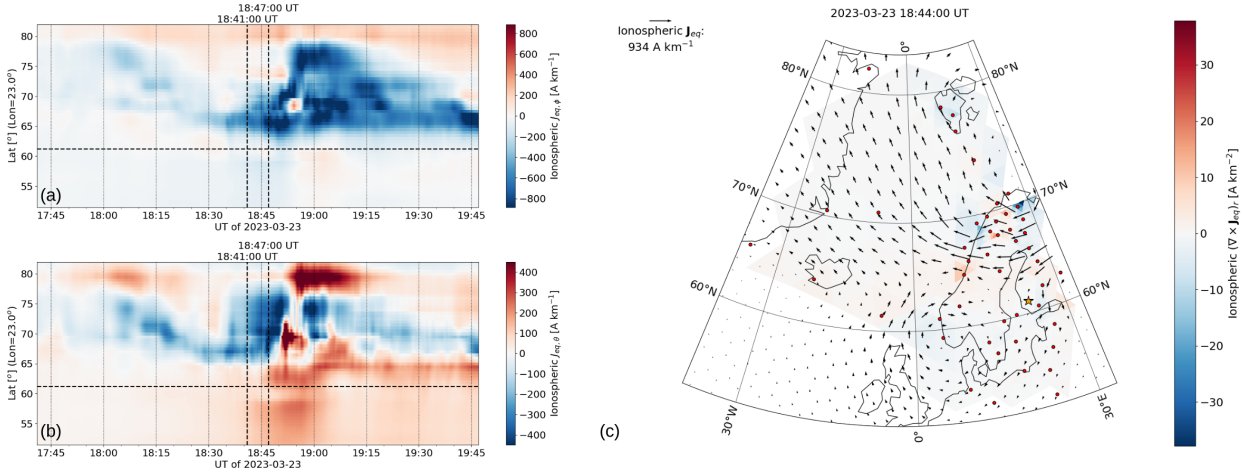

Figure 10. Equivalent current analysis applied to dune observations in the Finnish sector during the 23 March 2023 event. Same format as Fig. 8.

sector was within the westward electrojet (Fig. 10a and 10c). However, it cannot be excluded that the dunes were present at an earlier time but were simply not observed.

These three examples reveal that, while dune aurora seems to favour eastward electrojet conditions to appear, it can also be seen within the westward electrojet. It is important to stress that, as the dunes are generally accompanied by brighter auroral displays, the spatio-temporal patterns in the electrojet currents likely reflect the dynamical changes in the active auroral structures rather than those of the dunes themselves.

4 Discussion

Before discussing the results obtained from this study in light of the existing literature, we should mention a few caveats related to the nature of our main dataset. First of all, while all the Skywarden observations used in this study have been visually inspected to validate the presence of dunes in at least one image, we cannot be entirely certain that the time stamps associated with each observations are accurate. However, practices are gradually being harmonised and the quality of the citizen science data is improving fast, thanks to at least three aspects. First, the administrators of social media groups dedicated to aurora chasing play a crucial role by sharing a wealth of knowledge and expertise on how to best document an aurora night. Second, the Skywarden moderators inspect the submitted reports and correct mistakes they identify. Third, citizen science data quality has been benefitting from initiatives aiming at coordinating citizen science efforts in auroral science around the world, such as the ARCTICS Aurora Field Guide and Handbook for Citizen Science (Herlingshaw et al., 2024) or the Aurorasaurus project (e.g. MacDonald et al., 2015; Kosar et al., 2018). The main limitations and mitigations we can identify with the used dune observation dataset are the following:

https://doi.org/10.5194/egusphere-2025-5374
Preprint. Discussion started: 16 December 2025

1. The time stamps associated with dune aurora observations may contain errors. In a few cases, it was possible to identify a one-hour offset between the logged observation time and the image time stamps, most probably due to the camera being kept in daylight saving time in winter or vice-versa. These offsets were corrected. For a handful of observations, the time had been indicated in the 12-hour format whereas the Skywarden submission form assumes a 24-hour format. Such cases were also easily identified and corrected. However, when some time stamps were too unclear, the corresponding observations were ignored in the part of the analysis highly sensitive to timing (i.e. calculation of MLT of the observations, determination of associated driving parameters and geomagnetic indices, and estimation of the duration of the dune events).

2. Skywarden being originally and still primarily a Finnish observation system, reports from Central and Southern Finland largely dominate the database. This induces a geographic bias which can be seen in e.g. the geomagnetic latitude distribution and in the monthly distribution of dune observations. Such a geographic bias may also be reflected in the distribution of driving conditions associated with the dunes, as the auroral oval needs to expand enough to be visible from Central and Southern Finland. However, an increasing number of reports have been submitted to Skywarden from other parts of the world, as the system is becoming more widely known.

3. Given that the dunes are difficult to image (they are low-contrast structures in the dim diffuse aurora), they are often overlooked, and hence they are likely under-reported. Often, when they have been identified by an observer who shares the information with their aurora chasing community, additional reports are submitted to Skywarden as photographers specifically search for dune signatures in their own images.

4. One must also keep in mind that the geomagnetic latitudes associated with dune observations are in fact those of the observer as they were photographing the aurora. The latitude of the dunes themselves may therefore differ by a few degrees, depending on the elevation at which the dunes were located when seen from the observer's location. A conservative estimate of the incurred error in geomagnetic latitude is that the true latitude of the dunes is within $\pm 4.2^\circ$ of the observer's latitude, assuming that they are at an elevation of at least 10° above the observer's horizon and that they lie at approximately 100 km altitude (Palmroth et al., 2020). Given that in most observations where dunes are visible the camera pointing is not aligned with the meridional (north–south) direction and the elevation of the dunes is higher than 10°, the geographic (and hence geomagnetic) latitude offset is likely within a narrower confidence interval.

Bearing these limitations in mind, it is clear that the dunes have been seen in multiple regions located predominantly in the subauroral zone, in both hemispheres. While their occurrence pattern is to a great extent consistent with that of aurora observations in general, it exhibits a few peculiarities that may help uncover the formation mechanism of dune aurora.

We first note that the monthly distribution of observed dune events exhibit differences from that of Skywarden aurora reports. Specifically, the month with the largest number of dune aurora events is October, and the months of February and September have notably few dune events given the occurrence rate of the auroral observations reported by the citizen scientists. While it is

https://doi.org/10.5194/egusphere-2025-5374
Preprint. Discussion started: 16 December 2025

possible that those anomalies bear large statistical uncertainties due to the somewhat limited number of dune events (56), this may highlight a possible need for specific conditions for the dunes to form, other than geomagnetic activity.

In a study of mesospheric bores at middle and low latitudes between 2013 and 2017 with airglow observations from the Suomi-NPP satellite, Su et al. (2018) found two peaks in their monthly distribution: March through May and October. At high latitudes (Tromsø, 69.6°N), Chauhan et al. (2024) used a ground-based airglow imager to study mesospheric frontal structures including bores between 2011 and 2015. Out of the 18 events they identified, the majority took place in December and January. One important note is that, in that study, only clear-sky nights without auroral activity were considered. The exclusion of nights with auroral activity may have led to a bias favouring the deep-winter months over the equinox periods which are typically more geomagnetically active (Russell and McPherron, 1973). Another extensive statistical study of mesospheric bores was carried out by Hozumi et al. (2019), who observed airglow with the Visible and near-Infrared Spectral Imager on board the International Space Station between September 2012 and August 2015. They looked at the distributions of 306 mesospheric bores as a function of month and local time and found that midlatitude (up to 55° geographic latitude) bores are more frequent during the winter months. Their interpretation is that mesospheric bore formation in this case is likely associated with mesospheric inversion layers produced by migrating tides with large temperature amplitudes at mesospheric heights. The comparison of our dune event monthly distribution with the results from those past studies suggests that, while some aspects are in agreement (e.g. a peak in mesospheric bore occurrence in October), the dunes likely form as the result of a complex combination of processes involving both geomagnetic activity and middle-atmospheric dynamics.

In fact, while the emphasis in previous dune aurora studies has been placed on the mesospheric bore as a candidate atmospheric wave playing a role in the formation of dunes (Palmroth et al., 2020; Grandin et al., 2021), other types of waves modulating the neutral density near 100 km altitude could also be envisaged. In a master's thesis, Seltveit (2022) investigated three dune aurora events observed by airglow imagers in Antarctica and on Svalbard. The analysis of their properties (distance between wavefronts and propagating speed) revealed that, in those cases, the dunes were much more likely to be associated with gravity waves than with mesospheric bores. Their cases, however, generally showed shorter duration compared to the 2016 dune event analysed in Grandin et al. (2021). The shorter durations in those cases suggest gravity wave activity, whereas the longer-lived 2016 event initially appeared more consistent with a mesospheric bore interpretation. Our new observational statistics indicate that the dune event durations can range from much less than an hour to multiple hours. This could suggest that in some cases (typically, shorter event durations) the dunes might be associated with gravity waves, whereas in other cases (typically, longer event durations) they might be associated with mesospheric bores. Meanwhile, climatological results for high latitudes in Antarctica showed that high-frequency gravity waves (periods shorter than 3 h) have minimal variance at the mesopause around equinoxes, implying reduced overall gravity wave activity due to weak filtering winds below 80 km (Beldon and Mitchell, 2010). In the northern hemisphere, a similar trend has been found, with high-frequency gravity wave activity being generally higher during the winter months and reduced in March and September (de Wit et al., 2015). This, combined with the monthly patterns in auroral occurrence, darkness hours, and cloudiness, could contribute to explain the monthly distribution of dune aurora reports.

https://doi.org/10.5194/egusphere-2025-5374
Preprint. Discussion started: 16 December 2025

The statistical analysis of the driving parameters associated with dune aurora observations has evidenced that, generally, the dunes are observed when the solar wind density and pressure are elevated compared to their distributions across all aurora observations reported in Skywarden. In addition, the IMF magnitude associated with dune events also tends to be higher than during typical auroral displays. This could imply either that the strong driving is in itself required for the dunes to form or that the dunes generally appear at latitudes equatorwards from the typical auroral oval and hence need the ovals to expand sufficiently for the precipitating particles to reach the region where the atmospheric background is adequate (presence of an atmospheric wave at the suitable altitude). A possible reason for the former hypothesis could be that a solar wind pressure pulse could lead to the right type of particle precipitation to occur. For instance, Fuselier et al. (2004) showed that solar wind pressure pulses can lead to subauroral proton precipitation on the dayside, sometimes extending to the dusk sector. In the nightside, Søraas et al. (2013) found that protons of tens to hundreds of kiloelectronvolts had their precipitating flux exhibit temporal variations matching those of the solar wind dynamic pressure, presumably in relation to electromagnetic ion cyclotron wave activity in the inner magnetosphere. In fact, as was already hypothesised in Grandin et al. (2021), it is possible that the precipitating particles leading to the diffuse aurora in which the dunes emerge are auroral protons. Ono et al. (1987) showed that when protons precipitate into the upper atmosphere, they produce secondary electrons which can in turn excite the atmospheric constituents, leading to diffuse green emission. This process typically occurs in the equatorward side of the auroral oval and mainly in the dusk sector, which corresponds very well with the location where dunes have been observed – at least when in connection to the eastward electrojet. More recently, Nishimura et al. (2022) found that secondary electrons resulting from proton precipitation could produce a mix of red and green diffuse auroral emissions in the pre-midnight subauroral zone, again consistent with where dunes are most commonly reported. Yet, to be fully conclusive, detailed analyses of individual events with, for instance satellite observations of precipitating particle fluxes or ground-based spectrometer measurements, are needed.

5 Conclusions

Using citizen scientist observations from the Skywarden database, we have carried out the first statistical studies of dune aurora events. Since 2000, a total of 289 dune aurora observations have been reported into Skywarden, corresponding to 56 individual events which were seen from Northern Europe, North America, Australia, and New Zealand. We have analysed the statistical distribution of dune events as a function of magnetic local time, geomagnetic latitude, driving conditions, and geomagnetic activity. For 17 dune aurora events observed by several photographers in Fennoscandia, we have applied the SECS method to derive the equivalent ionospheric currents associated with each event.

The conclusions of our study are as follows:

1. The dunes can be observed in various regions of the world, predominantly at subauroral latitudes. This was already suggested in Grandin et al. (2024) but relied on self-reported observations without image-based verification.

2. A given dune event can be observed across a broad region and last for several hours, indicating that the event studied in Grandin et al. (2021) is not unique in that respect.

https://doi.org/10.5194/egusphere-2025-5374
Preprint. Discussion started: 16 December 2025

3. There does not seem to be any specific type of solar wind driver to produce dunes, though they are generally associated with moderately enhanced parameters, especially solar wind density and IMF magnitude, and the IMF B_y component might play a role in their formation. They are seen throughout the various phases of the solar cycle. Their latitudinal distribution shows some degree of correlation with geomagnetic activity, consistent with auroral oval expansion (SMR) and auroral activity (SME).

4. The monthly distribution of dune events is consistent with that of auroral observations, but with a notable difference in the northern-hemisphere autumn equinox (all-aurora event peak in September but dune aurora event peak in October). This difference may partly be explained by a lack of darkness in the early evening hours in September, but may also be related to the monthly distribution of atmospheric waves near the mesopause, or to some other cause yet to be determined.

5. The MLT distribution of dune observations peaks at an earlier local time than for all aurora observations, suggesting that the dunes might be associated with duskside processes. This could hint at a possible role of precipitating protons.

6. Dune aurora is associated with strong auroral electrojet signatures in ground-based magnetometer data. In most cases, the dunes are colocated with the eastward electrojet, but several cases correspond to the westward electrojet. The Harang discontinuity appears to be present in the immediate vicinity of the dunes.

Future work will aim at investigating in more detail the possible role of precipitating protons by analysing dune aurora events where supporting satellite and optical ground-based observations are available.

Data availability. The raw data used to set up the list of dune aurora observations between 1 January 2000 and 30 June 2025 were obtained from the Skywarden/Taivaanvahti API with the following command: https://www.taivaanvahti.fi/app/api/search.php?format=html&language=en&start=2000-01-01&end=2025-06-30&category=revontuli&detail_exact=dunes&with_images=1&columns=id,user,start_utc,city,latitude,longitude,details&format=csv. The list of visually validated observations for the purpose of this study will be deposited in a FAIR repository and cited here prior to publication.

The list of all aurora observations in Skywarden/Taivaanvahti between 1 January 2000 until 30 June 2025 can be retrieved with the following command: https://www.taivaanvahti.fi/app/api/search.php?format=html&language=en&start=2000-01-01&end=2025-06-30&category=revontuli&columns=id,user,start_utc,city,latitude,longitude,details&format=csv.

The SuperMAG magnetic index data (Gjerloev, 2012; Newell and Gjerloev, 2011, 2012) are available at https://supermag.jhuapl.edu (last access: 31 October 2025).

IMAGE data are available at https://space.fmi.fi/image/ (last access: 31 October 2025). The code for the SECS method is available as a supplement to Vanhamäki and Juusola (2020).

The cloudiness data across Finland for years 2015-2025 were obtained through the Finnish Meteorological Institute's open data API: https://en.ilmatieteenlaitos.fi/download-observations (last access: 31 October 2025).

https://doi.org/10.5194/egusphere-2025-5374
Preprint. Discussion started: 16 December 2025

Appendix A: List of the observers whose dune aurora observations reported in Skywarden were used in this study

Aki Karjalainen, Allison Mills, Andrew Clark, Ann-Marie Norlen, Anna Jansson, Anssi Mäntylä, Antero Ohranen, Antti Rinne, Arto Oksanen, Atacan Ergin, Berit Olsson, Bob King, Catharina Nilsson, Christina Sharp, Colin Legg, Cristina Casplin, Cristofer Eriksson, Danny Reardon, Donna Lach, Eero Karvinen, Eila Tiirinen, Elenore Olsson, Elizabeth Miller, Elizabeth Palmer, Ellis Judson, Emma Bruus, Erik Nyberg, Erkki Rauhala, Esa Pekka Isomursu, Fran Davis, Geir T. Birkeland Øye, Geoff Purchase, Graeme Whipps, Hanna Nilsson, Heidi Rikala, Heikki Jokiranta, Heikki Rantala, Heini Kulmala, Helen L. Chick, Ian Griffin, Iweta Seppälä, Jacqueline Guilford, Jan van den Brom, Jani Laasanen, Jani Lappalainen, Jani Lauanne, Janne Laukkanen, Jari Rajala, Jari Virtanen, Jari Ylioja, Jarkko Alatalo, Jarmo Leskinen, Jennifer Mainka, Jess Burrows, Jesse Kyytinen, Jessica Miller, Jim Perdue, Joanna Herranen, Johan Lundström, Johanna Amnelin, John Andersen, Jorma Mäntylä, Jouni Lehtola, Jouni Raunio, Jouni Riihelä, Ju-Kai Tsai, Juhani Hokkanen, Jukka Hilska, Jukka Kytömäki, Jukka Könönen, Jussi Muukka, Kaj Höglund, Kari Haila, Kari Rytilahti, Kari Saari, Kata Sivunen, Kathy Goltz, Kerry Saward, Kimmo Kantola, Kirsi Nikkola, Kjetil Vinorum, Kris Kidd, Kristina Saunders, Leena Aijasaho, Leo Jussila, Les Ladbrook, Lone Athanasakis, Lynette Mackenzie, Malin Englund, Mari Jääskeläinen, Maria Rönni, Markku Heikkinen, Markku Lintinen, Markku Ruonala, Markku Siljama, Markku Sirén, Marko Haapala, Marko Vallius, Marko Vesapuisto, Markus Hotakainen, Matias Takala, Matthew Bissett, Matti Helin, Matti T. Salo, Mauri Korpi, Megan Thomas, Michael Estwik, Michele Aucello, Michele Sadauskas, Mika Yrjölä, Mikael Johansson, Mikko Ankelo, Mikko Peussa, Mikko Silvola, Minna Glad, Minna Koivisto, Minna Lehtimäki, Minna Wires, Nick Keizerwaard, Olli Mantikka, Olli Reijonen, Pasi Tuomainen, Pauli Sorsakari, Pentti Arpalahti, Perttu Nihtila, Peter von Bagh, Petri Kuossari, Petri Martikainen, Petri Sallinen, Pia Simonen, Pirjo Koski, Raija Kokkola, Rami Valonen, Richard Dunstan, Risto Ennevaara, Rita Baker, Roope Luukkainen, Sakari Ekko, Sami Vähätalo, Samuli Ikäheimo, Santtu Pennanen, Sari Hukka, Sari Pietikäinen, Satu Juvonen, Satu Rajamäki, Shellie Evans, Simon Brandt, Sirpa Pursiainen-Hautala, Stella Rodriguez, Susanne Olsson, Tapio Nylund, Tapio Terenius, Teppo Laitinen, Terhi Törmälä, Tero Sipinen, Therese Forsberg, Timo Alanko, Timo Kantola, Timo Oksanen, Toby Schrapel, Tom Eklund, Tomi Katajamäki, Tommy Lågland, Toni Veikkolainen, Tuija Liunala, Tyler Benson, Ulf Jonsson, Ulla Vornanen, Ulrika Ivergård, Veikko Mäkelä, Vesa Puistovaara, Vesa Särkelä, Vesa Toropainen, Vesa Vauhkonen, Virpi Kauko, Yu Ahu; as well as four anonymous observers.

Appendix B: Cloudiness statistics in Finland

The monthly average nighttime cloudiness in Finland, between years 2015–2025, was calculated from the Finnish Meteorological Institute (FMI)'s open data nighttime cloud-okta measurements. Nighttime is defined when the solar elevation at ground level at a given meteorological station is at least 10° below the horizon (i.e. the solar zenith angle is greater than 100°).

First, we retrieved the hourly weather data from the FMI open data application programming interface (API) (https://en.ilmatieteenlaitos.fi/open-data) for each day during years 2015–2025, for all weather stations within latitudes comprised between 59 and 71°N and longitudes comprised between 20 and 32°E. Then, we retained the cloud-okta measurements corresponding to nighttime hours for the given stations, and finally we collected these cloud-okta values into monthly bins and calculated averages within each bin.

https://doi.org/10.5194/egusphere-2025-5374
Preprint. Discussion started: 16 December 2025

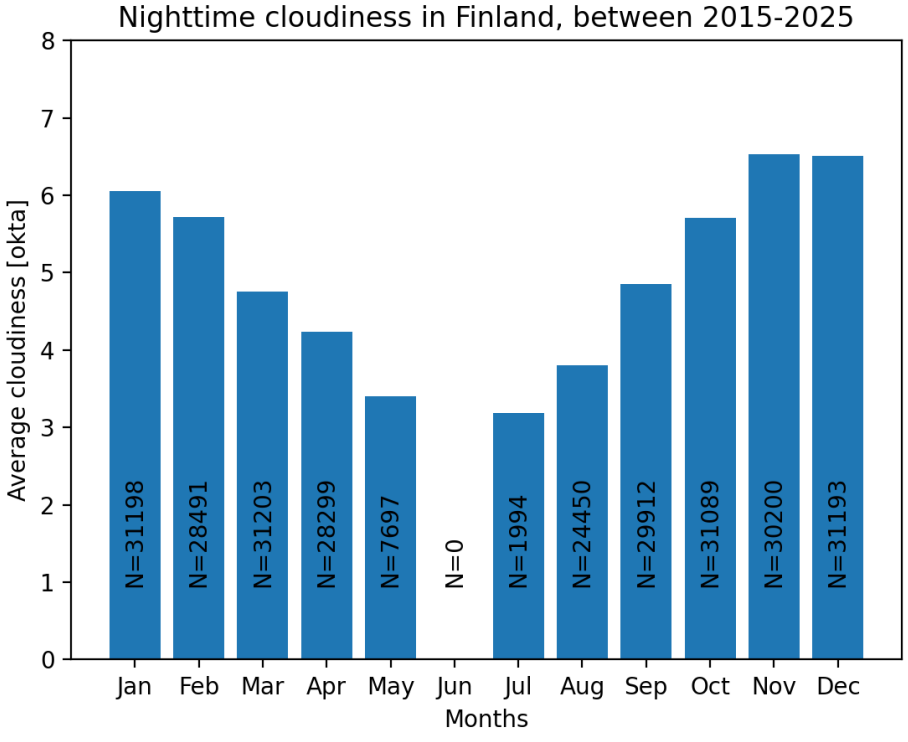

Figure B1. Average nighttime cloudiness (expressed in okta) for each month over Finland based on the Finnish Meteorological Institute's open data during 2015–2025. Nighttime hours are defined when the Sun's elevation is at least 10° below the horizon (i.e. solar zenith angle greater than 100°). The number of nighttime hours contributing to a given month's statistics is indicated in the corresponding bar of the diagram.

https://doi.org/10.5194/egusphere-2025-5374
Preprint. Discussion started: 16 December 2025

Author contributions. MG designed the study, carried out most of the data analysis, and wrote most of the manuscript. LJ carried out the equivalent current analysis and contributed with text to Sect. 2.4 and 3.4. JR and EB carried out the statistical analysis of cloudiness in Finland presented in Appendix B. DL provided the original photograph shown in Fig. 1. All co-authors have read the manuscript and provided comments to improve it.

Competing interests. The authors declare that they have no competing interests.

Acknowledgements. The authors wish to thank the 178 named and 4 anonymous citizen scientists who submitted dune observation reports to the Skywarden observation system (see the list of names in Appendix A). We also thank the Ursa Astronomical association for developing and maintaining Skywarden, as well as the moderators who check the submissions. MG expresses special thanks to Les Ladbrook (Aurora Australis (NZ)), Margaret Sonnermann (Aurora Australis Tasmania), Nick Bull (Aurora Hunters UK & Iceland), Donna Lach & Alysa Ferguson (Manitoba Aurora Chasers), and Tom Egil Dørum (Northern Lights (Nordlys) - www.nordlysvarsel.com) for sharing the call to report dune aurora observations to Skywarden via the aurora chaser Facebook groups they are administrating.

We thank the institutes who maintain the IMAGE Magnetometer Array: Tromsø Geophysical Observatory of UiT the Arctic University of Norway (Norway), Finnish Meteorological Institute (Finland), Institute of Geophysics Polish Academy of Sciences (Poland), GFZ German Research Centre for Geosciences (Germany), Geological Survey of Sweden (Sweden), Swedish Institute of Space Physics (Sweden), Sodankylä Geophysical Observatory of the University of Oulu (Finland), DTU Technical University of Denmark (Denmark), and Science Institute of the University of Iceland (Iceland). The provisioning of data from AAL, GOT, HAS, NRA, VXJ, FKP, ROE, BFE, BOR, HOV, SCO, KUL, and NAQ is supported by the ESA contracts number 4000128139/19/D/CT as well as 4000138064/22/D/KS.

This research was supported by the International Space Science Institute (ISSI) in Bern, Switzerland, through ISSI Working Group project ARCTICS. We gratefully acknowledge the SuperMAG collaborators (http://supermag.jhuapl.edu/info/?page=acknowledgement). We acknowledge use of NASA/GSFC's Space Physics Data Facility's OMNIWeb service, and OMNI data. The Scientific colour maps `turku` and `romaO` (Crameri, 2023) are used in this study to prevent visual distortion of the data and exclusion of readers with colour-vision deficiencies (Crameri et al., 2020).

MG acknowledges funding from the Research Council of Finland (grant 360433-ANAON) and from the European Union (ERC Starting Grant, LOUARN, 101161971). Views and opinions expressed are however those of the authors only and do not necessarily reflect those of the European Union or the European Research Council. Neither the European Union nor the granting authority can be held responsible for them. EB wishes to thank the Research Council of Finland for the support through grant 365202. EK acknowledges the Magnus Ehrnrooth Foundation for a travel grant to attend the ISSI meetings in Bern on 3–7 June 2024 and on 5–9 May 2025, and DL thanks the University of Calgary for the travel support to attend these meetings.

https://doi.org/10.5194/egusphere-2025-5374
Preprint. Discussion started: 16 December 2025

References

Amm, O.: Ionospheric Elementary Current Systems in Spherical Coordinates and Their Application., Journal of Geomagnetism and Geoelectricity, 49, 947–955, https://doi.org/10.5636/jgg.49.947, 1997.

Archer, W. E., Gallardo-Lacourt, B., Perry, G. W., St. -Maurice, J. P., Buchert, S. C., and Donovan, E.: Steve: The Optical Signature of Intense Subauroral Ion Drifts, Geophysical Research Letters, 46, 6279–6286, https://doi.org/10.1029/2019GL082687, 2019.

Beldon, C. L. and Mitchell, N. J.: Gravity wave-tidal interactions in the mesosphere and lower thermosphere over Rothera, Antarctica (68°S, 68°W), Journal of Geophysical Research (Atmospheres), 115, D18 101, https://doi.org/10.1029/2009JD013617, 2010.

Brown, L. B., Gerrard, A. J., Meriwether, J. W., and Makela, J. J.: All-sky imaging observations of mesospheric fronts in OI 557.7 nm and broadband OH airglow emissions: Analysis of frontal structure, atmospheric background conditions, and potential sourcing mechanisms, Journal of Geophysical Research (Atmospheres), 109, D19 104, https://doi.org/10.1029/2003JD004223, 2004.

Bruus, E.: Taivaanvahti/Himlakollen/Skywatcher's search interface, https://www.taivaanvahti.fi/app/docs/interface/output_interface_en.html, (last accessed: December 15, 2025), 2024.

Burrell, A., van der Meeren, C., and Laundal, K. M.: aburrell/aacgmv2: Version 2.6.0 [Software], Zenodo, https://doi.org/10.5281/zenodo.3598705, 2020.

Chauhan, N., Shiokawa, K., Gurubaran, S., Nozawa, S., Oyama, S.-i., and Nakamura, T.: Occurrence of Mesospheric Frontal Structures Over the High Latitude Station, Tromsø, Norway, Journal of Geophysical Research (Space Physics), 129, e2023JA032 243, https://doi.org/10.1029/2023JA032243, 2024.

Crameri, F.: Scientific colour maps v8.0.1 [Software], Zenodo, https://doi.org/10.5281/zenodo.8409685, 2023.

Crameri, F., Shephard, G. E., and Heron, P. J.: The misuse of colour in science communication, Nature Communications, 11, 5444, https://doi.org/10.1038/s41467-020-19160-7, 2020.

de Wit, R. J., Hibbins, R. E., and Espy, P. J.: The seasonal cycle of gravity wave momentum flux and forcing in the high latitude northern hemisphere mesopause region, Journal of Atmospheric and Solar-Terrestrial Physics, 127, 21–29, https://doi.org/10.1016/j.jastp.2014.10.002, 2015.

Dewan, E. M. and Picard, R. H.: Mesospheric bores, Journal of Geophysical Research, 103, 6295–6306, https://doi.org/10.1029/97JD02498, 1998.

Dewan, E. M. and Picard, R. H.: On the origin of mesospheric bores, Journal of Geophysical Research, 106, 2921–2927, https://doi.org/10.1029/2000JD900697, 2001.

Fuselier, S. A., Gary, S. P., Thomsen, M. F., Claflin, E. S., Hubert, B., Sandel, B. R., and Immel, T.: Generation of transient dayside subauroral proton precipitation, Journal of Geophysical Research (Space Physics), 109, A12 227, https://doi.org/10.1029/2004JA010393, 2004.

Gjerloev, J. W.: The SuperMAG data processing technique, Journal of Geophysical Research (Space Physics), 117, A09 213, https://doi.org/10.1029/2012JA017683, 2012.

Gonzalez, W. D., Joselyn, J. A., Kamide, Y., Kroehl, H. W., Rostoker, G., Tsurutani, B. T., and Vasyliunas, V. M.: What is a geomagnetic storm?, Journal of Geophysical Research, 99, 5771–5792, https://doi.org/10.1029/93JA02867, 1994.

Grandin, M., Palmroth, M., Whipps, G., Kalliokoski, M., Ferrier, M., Paxton, L. J., Mlynczak, M. G., Hilska, J., Holmseth, K., Vinorum, K., and Whenman, B.: Large-Scale Dune Aurora Event Investigation Combining Citizen Scientists' Photographs and Spacecraft Observations, AGU Advances, 2, e00 338, https://doi.org/10.1029/2020AV000338, 2021.

https://doi.org/10.5194/egusphere-2025-5374
Preprint. Discussion started: 16 December 2025

Grandin, M., Bruus, E., Ledvina, V. E., Partamies, N., Barthelemy, M., Martinis, C., Dayton-Oxland, R., Gallardo-Lacourt, B., Nishimura, Y., Herlingshaw, K., Thomas, N., Karvinen, E., Lach, D., Spijkers, M., and Bergstrand, C.: The Gannon Storm: citizen science observations during the geomagnetic superstorm of 10 May 2024, Geoscience Communication, 7, 297–316, https://doi.org/10.5194/gc-7-297-2024, 2024.

Grandin, M., Ledvina, V. E., Musset, S., Partamies, N., Frissell, N. A., Bruus, E., Nicoll, K. A., Mkrtchyan, H., Gallardo-Lacourt, B., Alfonsi, L., Jonassen, M. O., Whiter, D., Herlingshaw, K., Enengl, F., Doornbos, E., Jia, J., Kosar, B., Evans, L. P., Haberle, V., Laundal, K. M., and Barthelemy, M.: Citizen Science in Space and Atmospheric Sciences: Opportunities and Challenges, Surveys in Geophysics, https://doi.org/10.1007/s10712-025-09888-6, 2025.

Hayakawa, H., Ebihara, Y., Mishev, A., Koldobskiy, S., Kusano, K., Bechet, S., Yashiro, S., Iwai, K., Shinbori, A., Mursula, K., Miyake, F., Shiota, D., Silveira, M. V. D., Stuart, R., Oliveira, D. M., Akiyama, S., Ohnishi, K., Ledvina, V., and Miyoshi, Y.: The Solar and Geomagnetic Storms in 2024 May: A Flash Data Report, The Astrophysical Journal, 979, 49, https://doi.org/10.3847/1538-4357/ad9335, 2025.

He, F., Yao, Z., Ni, B., Cao, X., Ye, S., Guo, R., Li, J., Ren, Z., Yue, X., Zhang, Y., Wei, Y., Zhang, X., and Pu, Z.: Sawtooth and dune auroras simultaneously driven by waves around the plasmapause, Earth and Planetary Physics, 7, 237–246, https://doi.org/10.26464/epp2023023, 2023.

Heelis, R. A. and Maute, A.: Challenges to Understanding the Earth's Ionosphere and Thermosphere, Journal of Geophysical Research (Space Physics), 125, e27 497, https://doi.org/10.1029/2019JA027497, 2020.

Herlingshaw, K., Lach, D., Dayton-Oxland, R., Bruus, E., Karvinen, E., Ledvina, V., Partamies, N., Grandin, M., Spijkers, M., Nishimura, Y., Knudsen, D., Ladbrook, L., Martinis, C., Gallardo-Lacourt, B., Dyer, A., Mielke, L., Ratzlaff, C., Evans, L., Helin, M., Kuzub, J., Barthelemy, M., Thomas, N., Glad, M., Donovan, E., Syrjäsuo, M., Cordon, S., Andersen, J., and Legg, C.: ARCTICS Aurora Field Guide and Handbook for Citizen Science, Zenodo, https://doi.org/10.5281/zenodo.13931939, 2024.

Holappa, L., Gopalswamy, N., and Mursula, K.: Explicit IMF B_y-Effect Maximizes at Subauroral Latitudes (Dedicated to the Memory of Eigil Friis-Christensen), Journal of Geophysical Research (Space Physics), 124, 2854–2863, https://doi.org/10.1029/2018JA026285, 2019.

Holappa, L., Robinson, R. M., Pulkkinen, A., Asikainen, T., and Mursula, K.: Explicit IMF B_y Dependence in Geomagnetic Activity: Quantifying Ionospheric Electrodynamics, Journal of Geophysical Research (Space Physics), 126, e29 202, https://doi.org/10.1029/2021JA029202, 2021.

Hozumi, Y., Saito, A., Sakanoi, T., Yamazaki, A., Hosokawa, K., and Nakamura, T.: Geographical and Seasonal Variability of Mesospheric Bores Observed from the International Space Station, Journal of Geophysical Research (Space Physics), 124, 3775–3785, https://doi.org/10.1029/2019JA026635, 2019.

Izvekova, Y. N., Popel, S. I., Morozova, T. I., and Kopnin, S. I.: Possible manifestation of dusty ionospheric plasmas during high-speed meteor showers, Icarus, 429, 116 383, https://doi.org/10.1016/j.icarus.2024.116383, 2025.

King, J. H. and Papitashvili, N. E.: Solar wind spatial scales in and comparisons of hourly Wind and ACE plasma and magnetic field data, Journal of Geophysical Research (Space Physics), 110, 2104, https://doi.org/10.1029/2004JA010649, 2005.

Kosar, B. C., MacDonald, E. A., Case, N. A., and Heavner, M.: Aurorasaurus Database of Real-Time, Crowd-Sourced Aurora Data for Space Weather Research, Earth and Space Science, 5, 970–980, https://doi.org/https://doi.org/10.1029/2018EA000454, 2018.

Lockwood, M., Owens, M. J., Brown, W., and Vázquez, M.: The 2024 May event in the context of auroral activity over the past 375 yr, Monthly Notices of the Royal Astronomical Society, 540, 3596–3624, https://doi.org/10.1093/mnras/staf827, 2025.

https://doi.org/10.5194/egusphere-2025-5374
Preprint. Discussion started: 16 December 2025

MacDonald, E. A., Case, N. A., Clayton, J. H., Hall, M. K., Heavner, M., Lalone, N., Patel, K. G., and Tapia, A.: Aurorasaurus: A citizen science platform for viewing and reporting the aurora, Space Weather, 13, 548–559, https://doi.org/https://doi.org/10.1002/2015SW001214, 2015.

MacDonald, E. A., Donovan, E., Nishimura, Y., Case, N. A., Gillies, D. M., Gallardo-Lacourt, B., Archer, W. E., Spanswick, E. L., Bourassa, N., Connors, M., Heavner, M., Jackel, B., Kosar, B., Knudsen, D. J., Ratzlaff, C., and Schofield, I.: New science in plain sight: Citizen scientists lead to the discovery of optical structure in the upper atmosphere, Science Advances, 4, eaaq0030, https://doi.org/10.1126/sciadv.aaq0030, 2018.

Nevanlinna, H. and Tanskanen, E. I.: Early auroral photography and observations at the Sodankylä Geophysical Observatory in Finland, 1927–1929, History of Geo- and Space Sciences, 15, 17–25, https://doi.org/10.5194/hgss-15-17-2024, 2024.

Newell, P. T. and Gjerloev, J. W.: Evaluation of SuperMAG auroral electrojet indices as indicators of substorms and auroral power, Journal of Geophysical Research (Space Physics), 116, A12 211, https://doi.org/10.1029/2011JA016779, 2011.

Newell, P. T. and Gjerloev, J. W.: SuperMAG-based partial ring current indices, Journal of Geophysical Research (Space Physics), 117, A05 215, https://doi.org/10.1029/2012JA017586, 2012.

Nishimura, Y., Bruus, E., Karvinen, E., Martinis, C. R., Dyer, A., Kangas, L., Rikala, H. K., Donovan, E. F., Nishitani, N., and Ruohoniemi, J. M.: Interaction Between Proton Aurora and Stable Auroral Red Arcs Unveiled by Citizen Scientist Photographs, Journal of Geophysical Research (Space Physics), 127, e30 570, https://doi.org/10.1029/2022JA030570, 2022.

Nitta, N. V., Mulligan, T., Kilpua, E. K. J., Lynch, B. J., Mierla, M., O'Kane, J., Pagano, P., Palmerio, E., Pomoell, J., Richardson, I. G., Rodriguez, L., Rouillard, A. P., Sinha, S., Srivastava, N., Talpeanu, D.-C., Yardley, S. L., and Zhukov, A. N.: Understanding the Origins of Problem Geomagnetic Storms Associated with "Stealth" Coronal Mass Ejections, Space Science Reviews, 217, 82, https://doi.org/10.1007/s11214-021-00857-0, 2021.

Ono, T., Hirasawa, T., and Meng, C. I.: Proton auroras observed at the equatorward edge of the duskside auroral oval, Geophysical Research Letters, 14, 660–663, https://doi.org/10.1029/GL014i006p00660, 1987.

Palmroth, M., Grandin, M., Helin, M., Koski, P., Oksanen, A., Glad, M. A., Valonen, R., Saari, K., Bruus, E., Norberg, J., Viljanen, A., Kauristie, K., and Verronen, P. T.: Citizen Scientists Discover a New Auroral Form: Dunes Provide Insight Into the Upper Atmosphere, AGU Advances, 1, e00 133, https://doi.org/10.1029/2019AV000133, 2020.

Palmroth, M., Grandin, M., Sarris, T., Doornbos, E., Tourgaidis, S., Aikio, A., Buchert, S., Clilverd, M. A., Dandouras, I., Heelis, R., Hoffmann, A., Ivchenko, N., Kervalishvili, G., Knudsen, D. J., Kotova, A., Liu, H.-L., Malaspina, D. M., March, G., Marchaudon, A., Marghitu, O., Matsuo, T., Miloch, W. J., Moretto-Jørgensen, T., Mpaloukidis, D., Olsen, N., Papadakis, K., Pfaff, R., Pirnaris, P., Siemes, C., Stolle, C., Suni, J., van den IJssel, J., Verronen, P. T., Visser, P., and Yamauchi, M.: Lower-thermosphere-ionosphere (LTI) quantities: current status of measuring techniques and models, Annales Geophysicae, 39, 189–237, https://doi.org/10.5194/angeo-39-189-2021, 2021.

Papitashvili, N. E. and King, J. H.: OMNI Hourly Data [Data set], NASA Space Physics Data Facility, https://doi.org/10.48322/1shr-ht18, 2020.

Partamies, N., Juusola, L., Tanskanen, E., and Kauristie, K.: Statistical properties of substorms during different storm and solar cycle phases, Annales Geophysicae, 31, 349–358, https://doi.org/10.5194/angeo-31-349-2013, 2013.

Pitkänen, T., Hamrin, M., Kullen, A., Maggiolo, R., Karlsson, T., Nilsson, H., and Norqvist, P.: Response of magnetotail twisting to variations in IMF B_y: A THEMIS case study 1-2 January 2009, Geophysical Research Letters, 43, 7822–7830, https://doi.org/10.1002/2016GL070068, 2016.

https://doi.org/10.5194/egusphere-2025-5374
Preprint. Discussion started: 16 December 2025

Rong, Z. J., Lui, A. T. Y., Wan, W. X., Yang, Y. Y., Shen, C., Petrukovich, A. A., Zhang, Y. C., Zhang, T. L., and Wei, Y.: Time delay of interplanetary magnetic field penetration into Earth's magnetotail, Journal of Geophysical Research (Space Physics), 120, 3406–3414, https://doi.org/10.1002/2014JA020452, 2015.

Russell, C. T. and McPherron, R. L.: Semiannual variation of geomagnetic activity, Journal of Geophysical Research, 78, 92, https://doi.org/10.1029/JA078i001p00092, 1973.

Sarris, T., Palmroth, M., Aikio, A., Buchert, S. C., Clemmons, J., Clilverd, M., Dandouras, I., Doornbos, E., Goodwin, L. V., Grandin, M., Heelis, R., Ivchenko, N., Moretto-Jørgensen, T., Kervalishvili, G., Knudsen, D., Liu, H.-L., Lu, G., Malaspina, D. M., Marghitu, O., Maute, A., Miloch, W. J., Olsen, N., Pfaff, R., Stolle, C., Talaat, E., Thayer, J., Tourgaidis, S., Verronen, P. T., and Yamauchi, M.: Plasma-Neutral Interactions in the Lower Thermosphere-Ionosphere: The need for in situ measurements to address focused questions, Frontiers in Astronomy and Space Sciences, 9, 435, https://doi.org/10.3389/fspas.2022.1063190, 2023.

Seltveit, S. H.: Auroral dunes: Bores or boring? Airglow imaging of gravity wave–aurora interaction in the mesosphere lower thermosphere, Master's thesis, NTNU – Norwegian University of Science and Technology, Trondheim, Norway, https://hdl.handle.net/11250/3033754, 2022.

Shepherd, S. G.: Altitude-adjusted corrected geomagnetic coordinates: Definition and functional approximations, Journal of Geophysical Research (Space Physics), 119, 7501–7521, https://doi.org/10.1002/2014JA020264, 2014.

Smith, S. M., Taylor, M. J., Swenson, G. R., She, C.-Y., Hocking, W., Baumgardner, J., and Mendillo, M.: A multidiagnostic investigation of the mesospheric bore phenomenon, Journal of Geophysical Research (Space Physics), 108, 1083, https://doi.org/10.1029/2002JA009500, 2003.

Søraas, F., Laundal, K. M., and Usanova, M.: Coincident particle and optical observations of nightside subauroral proton precipitation, Journal of Geophysical Research (Space Physics), 118, 1112–1122, https://doi.org/10.1002/jgra.50172, 2013.

Spogli, L., Alberti, T., Bagiacchi, P., Cafarella, L., Cesaroni, C., Cianchini, G., Coco, I., Di Mauro, D., Ghidoni, R., Giannattasio, F., Ippolito, A., Marcocci, C., Pezzopane, M., Pica, E., Pignalberi, A., Perrone, L., Romano, V., Sabbagh, D., Scotto, C., Spadoni, S., Tozzi, R., and Viola, M.: The effects of the May 2024 Mother's Day superstorm over the Mediterranean sector: from data to public communication, Annals of Geophysics, 67, PA218, https://doi.org/10.4401/ag-9117, 2024.

Su, Y., Yue, J., Liu, X., Miller, S. D., Straka III, W. C., Smith, S. M., Guo, D., and Guo, S.: Mesospheric Bore Observations Using Suomi-NPP VIIRS DNB during 2013-2017, Remote Sensing, 10, 1935, https://doi.org/10.3390/rs10121935, 2018.

Vadas, S. L. and Becker, E.: Numerical Modeling of the Generation of Tertiary Gravity Waves in the Mesosphere and Thermosphere During Strong Mountain Wave Events Over the Southern Andes, Journal of Geophysical Research (Space Physics), 124, 7687–7718, https://doi.org/10.1029/2019JA026694, 2019.

Vadas, S. L. and Liu, H.-l.: Generation of large-scale gravity waves and neutral winds in the thermosphere from the dissipation of convectively generated gravity waves, Journal of Geophysical Research (Space Physics), 114, A10 310, https://doi.org/10.1029/2009JA014108, 2009.

Vanhamäki, H. and Juusola, L.: Introduction to Spherical Elementary Current Systems, in: Ionospheric Multi-Spacecraft Analysis Tools, pp. 5–33, ISSI Scientific Report Series 17, https://doi.org/https://doi.org/10.1007/978-3-030-26732-2_13, 2020.

Weygand, J. M. and Wing, S.: Comparison of DMSP and SECS region-1 and region-2 ionospheric current boundary, Journal of Atmospheric and Solar-Terrestrial Physics, 143–144, 8–13, https://doi.org/https://doi.org/10.1016/j.jastp.2016.03.002., 2016.

Weygand, J. M., Ngwira, C. M., and Arritt, R. F.: The Equatorward Boundary of the Auroral Current System During Magnetic Storms, Journal of Geophysical Research (Space Physics), 128, e2023JA031 510, https://doi.org/10.1029/2023JA031510, 2023.

https://doi.org/10.5194/egusphere-2025-5374
Preprint. Discussion started: 16 December 2025

Zhang, Y., Sun, W., Feng, X. S., Deehr, C. S., Fry, C. D., and Dryer, M.: Statistical analysis of corotating interaction regions and their geoeffectiveness during solar cycle 23, Journal of Geophysical Research (Space Physics), 113, A08 106, https://doi.org/10.1029/2008JA013095, 2008.